The University Of Sheffield.

Department Of Mechanical Engineering

Mechanical Engineering

Master of Philosophy Thesis

Comparison of two musculoskeletal models to evaluate glenohumeral joint kinematics and dynamics

Adrian Elias

April 2022

Supervisors

Prof. Claudia Mazzà

Dr. Xinshan Li

Acknowledgments

I am grateful to my lovely family (Axel, Augusto, and Mirna) that supported me for my research during this pandemic. I would like to express my gratitude to my supervisors Claudia Mazzà and Xinshan Li, and my sponsor in Mexico, CONACYT. I acknowledge the contribution of my tutors and mentors: Paul Barnes, Dalbinder Kular, Kathrin Fradley and Rachael Staves for their support to help me improve my writing and academic skills. Furthermore, this research would not be possible without the support of the Integrative Musculoskeletal Biomechanics Group, specially to Erica Montefiori and Claude Hayford This research could not be possible without the help of Claudia Romero Jorge Bosch and Rodolfo Vilchis, Rodrigo Lechuga and Ulises Serratos that guided me to improve my mathematical and programming skills.

Summary

The musculoskeletal models have been used to estimate simultaneously the internal forces and the joint kinematics during motion to avoid intrusive methods to diagnose glenohumeral instability. The Holzbaur model and the Wu model have the main algorithms to calculate the joint kinematics and dynamics that are used in most of the musculoskeletal models to evaluate mobility and instability. No research has been done to compare the two main shoulder models' algorithms to evaluate shoulder mobility and have been reported to evaluate stability. The estimation of range of motion and the joint reaction forces are fundamental to find quantitative parameters to evaluate stability and mobility. The shoulder mobility has been evaluated with standardized motion. From these, standardized motions, abduction has been used as a clinical test to evaluate kinematic patterns to differentiate from healthy subjects and subjects with anterior-posterior instability. Nevertheless, the lack of evidence of the comparison of both models has not been enough to find what model is better to evaluate joint kinematics and dynamics. The joint kinematics and dynamics are essential to differentiate between healthy and pathological subjects. Through the use of musculoskeletal models, the computation algorithms are used to estimate the joint joint kinematics, moments, and joint contact forces that are calculated based on experimental data. Nevertheless, the musculoskeletal models need to be ranked, and evaluated with experimental data to identify the best models to evaluate joint kinematics and dynamics. The direct measurement of joint reaction forces with biomodular implants [1] are essential to compare the joint reaction forces that are estimated with both models. The biomodular implants have been evaluated in patients with total shoulder replacement to have a better approach to estimate the joint contact forces with musculoskeletal models. The comparison of musculoskeletal models will help to evaluate joint kinematics and dynamics for healthy subjects and patients with other surgical procedures. This research is designed to verify the models' capability to estimate joint contact forces with the aim of improving the accuracy to improve the detection of quantitative parameters to assess glenohumeral joint instability.

The diagnosis of glenohumeral joint instability has been quantified with the estimation of joint kinematics and dynamics with musculoskeletal models. The comparison of the joint reaction forces between the two models can improve the methods to detect the algorithm's ability to evaluate glenohumeral instability and other motion related pathologies.

Eight participants were requested to realize three cycles of 90-degree thoracohumeral elevation with a three second isometric motion that was guided with a digital metronome. Cartesian coordinates of the bony landmarks were obtained to estimate 3 degrees of freedom of rotations for the shoulder joint. The joint moments and joint reaction forces were estimated and compared with direct measurement of joint moments and joint rection forces measured with biomodular implants found in the literature [2,3,4].

The main angle of rotation was the thoracohumeral elevation. The complementary angles are the shoulder rotation and the thoracohumeral plane angle. The findings of this research are that the main differences in the standard deviation between the Wu and Holzbaur model are detected in the midrange of the thoracohumeral plane and shoulder rotation angles which proves that the differences in algorithms with both models have as a result different output for the joint kinematics and the internal forces. and with the use of controlled conditions for the joint kinematics data in further research. The use of biomodular implants with the measurement of joint kinematics has been the best method to compare the joint moments and joint rection forces between the biomodular implants and the musculoskeletal models[2]. Nevertheless, the statical analysis done in this research recommends the analysis with a higher sample of participants with biomodular implants that execute motion with a simultaneous capture of the kinematic data.

Content

Abbreviation

Acromioclavicular (AC)

Degree of Freedom (DOF)

Humeroclavicular (HC)

Sternoclavicular (SC)

Glenohumeral (GH)

Glenohumeral Joint (GHJ)

Glenohumeral Joint Instability (glenohumeral joint instability)

Glenohumeral Joint translations (glenohumeral joint translations)

Joint reaction Force (JRF)

Glenohumeral Joint reaction force (GHJRF)

Suprahumeral (SH)

Thora scapular (TS) or Scapulothoracic (ST)

Thoracohumeral (TH)

Multidirectional instability (MDI)

Magnetic Resonance Image (MRI)

Computer tomography (CT)

Motion Capture System (MOCAP)

Musculoskeletal (MSK)

Glenohumeral reaction force (GHRF)

Linear Displacement Transducer (LDTS)

X-ray computed tomography (x-ray CT)

Electron beam computed tomography (EBCT)

Scapular Rhythm (scapular rhythm)

Inverse Kinematics (IK)

Physiological Cross-Sectional Area (PCSA)

Global Optimisation Method (GOM)

Coordinate Limit force (CLF)

Force directed kinematics (FD)

1 INTRODUCTION

The complexity of the shoulder in motion has been studied to improve the effectiveness of interventions with patients with shoulder pathologies. The challenge of evaluating shoulder pathologies is to accurately differentiate between healthy and pathological subjects. The motion of the shoulder has been proven to provide accurate information of shoulder pathologies. Shoulder motion patterns are the description of motion that help identify pathological patterns of motion from healthy patterns of motion. Therefore, the main problem in research is to find the best method to evaluate shoulder motion patterns for different pathologies. For the glenohumeral joint, the most important challenge is to measure accurately the joint kinematics and dynamics to evaluate shoulder motion patterns.

1.1 **Anatomy**

Understanding the anatomy of the shoulder and the glenohumeral joint is essential to understand the interaction between all the anatomical structures in the shoulder that interact during motion. The shoulder is comprised of four bones: scapula, thorax, clavicle, and humerus. The four bones have seven anatomical structures, which are the regions described in Figure 1 ,(Sternum, ribs, clavicle, scapula, acromion, humerus and glenoid). The definitions of the anatomical structures are relevant because they are regions where muscles are inserted to have contact between the anatomical structures. The classification of joints and anatomical structures is based on previous research that involve all the muscles that interact in the shoulder, based on the origin and insertion of the muscles[5]. The seven anatomical structures are linked with seven anatomical joints (glenohumeral, suprahumeral, acromioclavicular, thoracohumeral, scapulothoracic, sternoclavicular and sternocostal) [6] that work together to provide motion to the shoulder, shown in Figure 1. Of all the joints, the glenohumeral joint (GHJ) has the largest range of motion of any major moveable joints in the human body. The GHJ is comprised of the glenoid (a shallow concave surface in the scapula) and the humerus[7].

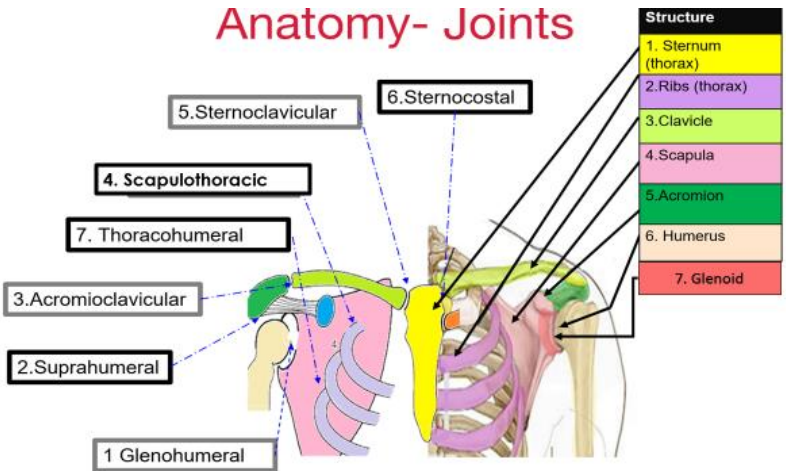

Figure 1. Shoulder joints based on [8] **and** [5]

Figure 2 shows the anterior, posterior, and sagittal views of the scapula. The GHJ has contact between the proximal end of the humeral head, the glenoid fossa and glenoid labrum (inner surface). The glenoid cavity (fossa) is described as "a depression in the lateral angle of the scapula that articulates with the humeral head"[9], marked with a red square in Figure 2. The humerus head has been reported to be up to three times bigger than the glenoid fossa, which is described as a size ratio 3:1. The size ratio between the humerus and glenoid facilitates the mobility of the GHJ. The size ratio between humerus and glenoid has been considered to be an important factor for instability[9].

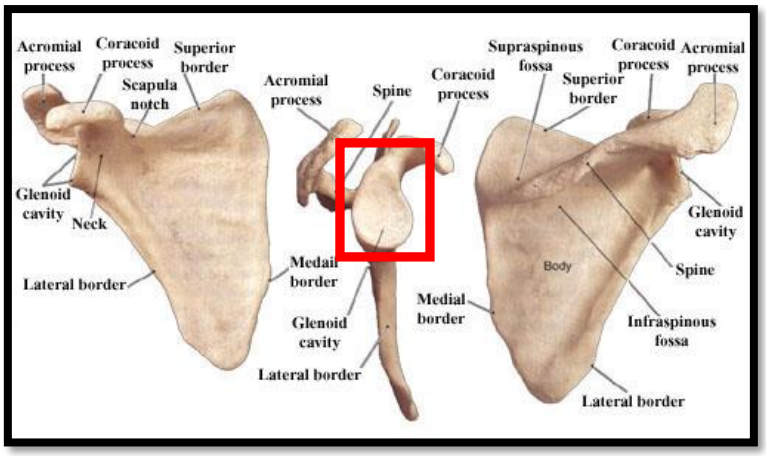

Figure 2. Anterior, lateral, and posterior views of the scapula [10]**.**

The GHJ is commonly assumed to be a ball and socket joint, with the humerus head being the ball and the glenoid being the socket. The labrum is a fibrocartilaginous ring that covers the glenoid (see Figure 3) [11,9]. The labrum increases the depth of the glenoid. The main function of the glenoid labrum is to use concavity- compression effects to maintain the position of the humerus centred to the glenoid fossa[12].

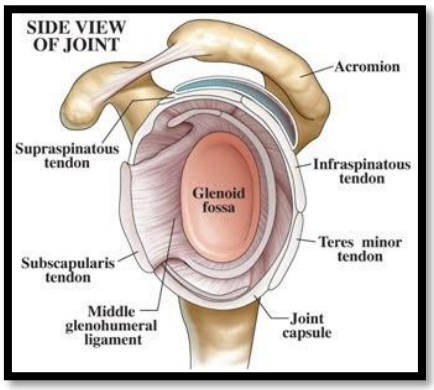

Figure 3. Glenoid fossa and labrum Copied from [10]

1.2 Glenohumeral joint instability

The GHJ provides stability and mobility to the humerus and the glenoid fossa of the scapula for the in static position and during motion of the shoulder joint [13]. Glenohumeral joint pathologies can significantly decrease mobility and/or stability of the shoulder. Glenohumeral joint disorders may affect a wide range of daily life activities, including eating and sleeping, but especially those involving overhead shoulder motions[14]. Glenohumeral instability is an abnormal movement, which exists when the humeral head does not remain centred with the glenoid fossa during motion[15]. Consequently, the glenohumeral instability generates pain and discomfort during daily life activities.

2 AIM AND OBJECTIVES

To compare the joint kinematics and kinetics of two musculoskeletal shoulder models to evaluate the best candidate to estimate joint reaction forces to improve the assessment of glenohumeral joint instability. s

The following objectives have been identified:

1. Capture shoulder motion kinematic data from a group of eight healthy volunteers with a motion capture optoelectronic system
2. Estimate the joint kinematics using two shoulder musculoskeletal models with OpenSim software
3. Compare joint kinematics of both models to evaluate the mobility of the shoulder joints
4. Compare the joint moments of both models
5. Estimate resultant glenohumeral joint reaction forces with the same two models
6. Compare the resultant glenohumeral joint reaction forces with literature data from an instrumented prosthesis to evaluate the accuracy of the musculoskeletal models

3 LITERATURE REVIEW

The main challenge for current research of glenohumeral joint instability is to improve the accuracy of the assessment of glenohumeral instability. The assessment of glenohumeral instability requires an accurate description of the motion of the glenohumeral joint and the muscle forces that generate motion. The description of the motion is essential to better understand the causes of glenohumeral joint instability. Therefore, this literature review will describe the existing methods to measure the joint kinematics and dynamics of the glenohumeral joint.

3.1 Glenohumeral function: mobility and stability

The GHJ needs to be stable and mobile to be functional for daily life activities. Researchers have designed methods to evaluate GHJ mobility [16,17] and stability. The methods to evaluate GHJ mobility evaluate the range of motion. As shown in Figure 4,There are two main standard movements to evaluate mobility that have been widely investigated in the literature: abduction and flexion [14,18,19].

Glenohumeral instability is detected when the net forces of the glenohumeral joint are not directed to the glenoid fossa during motion. Anterior-posterior instability occurs when the joint reaction forces are not aligned in the anterior-posterior direction during motion. The anterior-posterior instability is the most common type of instability, that is evaluated in shoulder abduction[20].

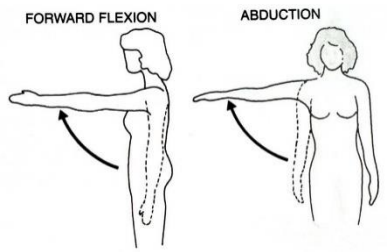

Figure 4.Shoulder Flexion (forward) and Abduction (thoracohumeral elevation)[21]

Scapular rhythm is the ratio of rotations between scapula and humerus relative to the thorax. Previous studies have used scapular rhythm as a functional evaluation of the shoulder joint's coordination [22,23]. Researchers measure shoulder mobility with the scapular rhythm [24,25,26] by quantifying the ability to coordinate complex motions in the shoulder joint. The scapular rhythm is measured with the ratio of glenohumeral rotation relative to scapulothoracic rotation during thoracohumeral elevation (showed in Figure 4). Scapular rhythm tests help detect a decrease in range of motion or a functional limitation. Scapular rhythm tests are also useful to detect motion related glenohumeral pathologies when compared with healthy subjects, for instance glenohumeral joint instability [27].

The differences in scapular rhythm between healthy and pathological subjects help with identifying the limitation of range of motion of scapula relative to thorax, and relative motion from scapula to humerus. In Figure 5 the main rotations are represented in a 2-dimensional plane for every joint: 'α' the glenohumeral angle,'β' the scapulothoracic angle and 'γ'the thoracohumeral angle. However, in reality, the motion of the shoulder occurs in a 3-dimensional space and every joint has three physiological rotations and translations. Therefore, 3D kinematic analysis is fundamental to detect pathologies with scapular rhythm [23,28,29]. Scapular rhythm helps to evaluate mobility and GHJ motion related pathologies, [22], and to understand the relationship between the range of motion and the glenohumeral joint instability [30].

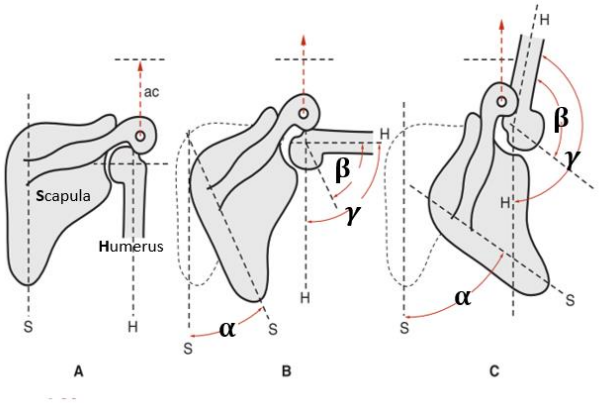

Figure 5. Angles between scapula, humerus and thorax in thoracohumeral elevation [31]

3.2 **Pathophysiology of glenohumeral joint instability**

In a stable GHJ the head of the humerus stays centred in the glenoid fossa thanks to the combined action of the rotator cuff and the capsule [32], as shown in Figure 6. The main passive stabilizers are the glenohumeral ligaments [33] that pull in the direction of vector 'D' shown in Figure 6. The passive and active stabilizers keep the GHJ stable, resulting in the humerus being centred in the glenoid fossa 'G' during motion.

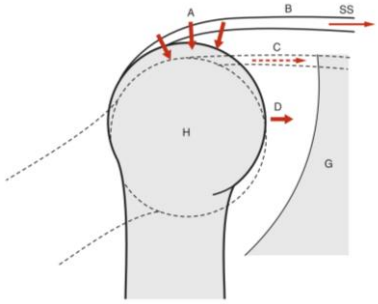

Figure 6. Humerus head and forces in the GHJ H (humerus head), G (glenoid Fossa), SS(supraspinatus), A (Gravity forces), D (active lateral displacement), B (conjoined tendon), C (Superior aspect of capsule) [12]

Muscles are the main active stabilizers, glenohumeral joint instability is caused by structural damage or a pathological imbalance of muscle forces during motion. For clinicians knowing the direction and degree of glenohumeral joint instability allows them to identify the cause of instability [34].

The direction and degree of glenohumeral joint instability is evaluated based on the direction of the glenohumeral joint translations and the degree of GHJ laxity. glenohumeral joint translation is defined as the relative displacement between humeral head and glenoid. Glenohumeral joint laxity is defined as a non-symptomatic degree of glenohumeral joint translations, that is described to be inside a normal non-pathological range [33]. According to some authors, the concept of glenohumeral joint instability has been misunderstood by researchers due to the fact that laxity and instability are not typically differentiated [35]. The confusion in definitions has generated an incorrect classification in patients [33]. The main difference between laxity and instability is that laxity is measured in static positions, whilst instability occurs during motion as shown in

Figure 7. Some authors have reported that glenohumeral laxity is crucial to diagnose instability [36,37], in contrast with other authors that claim that there is no causality between

laxity and instability [33,38]. The GHJ laxity is an important risk factor in glenohumeral joint instability, but it has not proven to be a determinant factor. Understanding the nature of the relationship between laxity and instability, requires a deep knowledge of the interaction of all the forces that are acting in the GHJ. Researchers have found that glenohumeral joint instability is highly influenced by muscle contractions [39,40,41]. The diagnosis of glenohumeral joint instability in static positions does not consider muscle contractions during motion and so it does not provide enough information to detect glenohumeral joint instability for daily life activities [33]. Therefore, to improve accuracy of diagnosis of glenohumeral joint instability, it is essential to evaluate glenohumeral joint translations during motion and kinematic patterns of the GHJ.

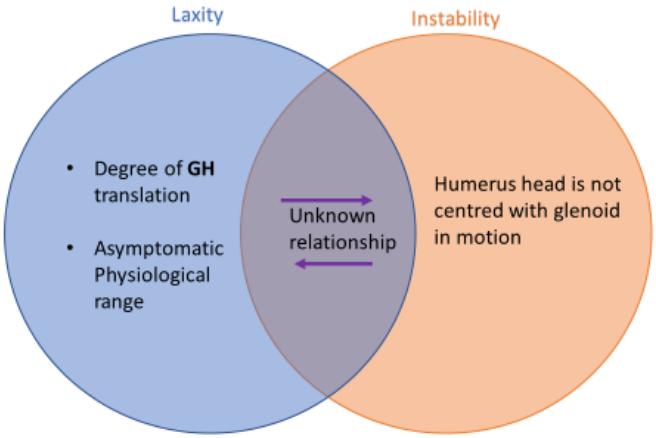

Figure 7. Laxity and instability based on [33]**.**

Even though researchers have discovered a gap in the relationship between laxity and instability [33], no research was found to fill this gap with objective quantitative parameters to improve the understanding of the relationship between laxity and instability. Instead of using objective quantitative parameters, Lewis[33], recommends a novel classification and recommends diagnostic arthroscopy as the only accurate method to detect glenohumeral joint instability. Other authors recommend the design of a subject-specific treatment due to the complexity in classification for every clinical presentation [20].

An existing gap in research is the lack of databases of GHJ kinematic patterns that provide quantitative parameters to detect glenohumeral joint instability. The lack of databases of GHJ kinematic patterns could be related to the lack of measurements of glenohumeral joint

translations in static and during motion with accurate methods [42]. Biomechanical assessment is essential to quantify the kinematic patterns to differentiate between healthy and pathological subjects.

3.2.1 **Clinical current practices**

The goal of a diagnosis is to understand the problem of the patient. The diagnostic process requires interdisciplinary collaboration and relies on the characteristics of each health care system. The diagnostic process requires iterations of clinical assessment to increase the precision of diagnoses. The diagnosis is essential to explain the problem to the patient and all the members of the interdisciplinary team of the healthcare system. Mistakes during clinical assessment can be propagated through inefficient collaboration and communication between clinicians, patients, and family members and could result in diagnostic errors. If an accurate diagnosis is not provided to clinicians, patients and the family members, this lack of precision could lead to harm to the patient [43]. Therefore, objective parameters are needed that are clear and precise and can be shared with patients and clinicians.

The evaluation of anatomical and functional components of the GHJ has been evaluated with several tests, nevertheless, the sensitivity and specificity reported by the authors has been inconsistent with the results. In contrast, the physical examination within a general history and a and specific shoulder history of the patient has been reported to be essential for diagnosing and managing any shoulder instability [15].

The specific shoulder history must include an evaluation that reports if there is signs of “instability, pain, stiffness, locking, catching, or swelling” [20]. Furthermore, the patient must report the family history of atraumatic instability and any evidence of hyperlaxity in the patient and family members. Physical examination of the unstable shoulder relies on generalized laxity tests [20]. Nevertheless, laxity is difficult to detect with physical examination. Patients with generalized and shoulder hyperlaxity do not always have pathological effects on the shoulder. The diagnosis of glenohumeral joint instability requires a set of tests to assess laxity, range of motion, strength, and the detection of functional problems. The comparison of these tests is more accurate when compared with the patient's healthy contralateral shoulder. A limitation of the comparison of both shoulders is that some patients can have injury in both shoulders or the lack of anatomical structures in the healthy shoulder [15].

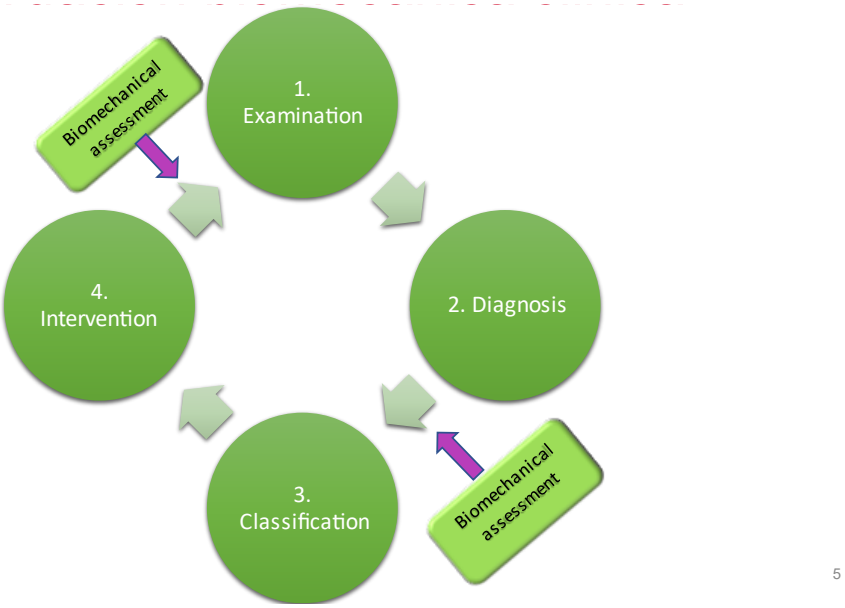

Figure 8. The role of biomechanical assessment in the clinical diagnosis

The diagnosis is evaluated with a clinical history and an examination. If the examination is accurate authors have reported that 90% of the cases are diagnosed correctly [33,44] . Nevertheless, physical examination with clinical manual tests has been proven not have enough reproducibility and repeatability to diagnose accurately the patients to classify accurately glenohumeral instability [34].. Therefore, researchers have designed biomechanical assessments to quantify the motion of the glenohumeral joint to improve the accuracy of examination and diagnosis. The biomechanical assessment aims to improve the accuracy of the classification of glenohumeral instability as shown in Figure 8.

3.2.2 Classification of Glenohumeral Instability and clinical assessment

Previous studies have highlighted the classification as the central step to define an intervention [33,45]. Several classification methods have been proposed to divide patients in groups and create a specific intervention depending on the causes of instability based in subjective parameters [15,45,46].

glenohumeral joint instability is classified by the degree of severity: starting with impingement, subluxation and the worst case, dislocation. Impingement is described as the compression of soft tissue between shoulder bones [47]. Patients with impingement are

described to have a moderate displacement of the humerus relative to the scapula. Nevertheless, “moderate” is only a subjective description of a complex pathology. Patients that are diagnosed with subluxation have been described to have an uncontrolled humerus translation without dislocation [33]. Other authors describe subluxation as the feeling of the humerus sliding in and out of the glenoid [20]. The most severe case of instability is the full humeral dislocation, which occurs when the humerus goes out the glenoid fossa. Impingement and subluxation have been defined with subjective parameters and have not been differentiated quantitatively with gold standard methods. Every author has generated different qualitative parameters to classify the degree of instability without a standardized convention Only subluxation has been quantified [48], but it interesting to note that the researchers have not differentiated quantitative parameters between subluxation and impingement. After evaluating definitions of glenohumeral joint instability , a current gap in classification methods is the lack of quantitative parameters to evaluate various classifications of instability over a period of time [33]. The consequences of this gap for patients, is that not all the clinical presentations have a correct diagnosis. If the diagnosis is not correct, the treatment may not be appropriate.

The current gap in classification has hampered a representative statistical analysis of impingement and subluxation. Only one degree has been globally recorded, glenohumeral dislocation. Glenohumeral dislocation has been reported to be the most common global glenohumeral injury with 11 to 51 cases for every 100,000 [49] [50,51]. There could be more cases of glenohumeral joint instability that are not reported such as subluxation or impingement [45], because these cases do not require hospitalization and therefore, are not frequently reported in medical centres.

Clinicians use manual tests to detect glenohumeral joint instability based on the glenohumeral motion shown in Figure 9. The tests detect if there is a ‘high’ relative displacement between humerus and scapula. The clinician tests the glenohumeral displacement with the application of a force to the humerus to detect the degree of humeral translation relative to the glenoid fossa in a vertical and a horizontal direction [20,34]. Researchers have explained the importance of measuring the 3 direction of glenohumeral joint translations to improve diagnosis [52]. A limitation in manual tests, is that one out of three directions of glenohumeral joint instability is not measured Therefore, this research will evaluate non-intrusive tools that can be candidates to evaluate the three directions to evaluate GHI.

The manual tests evaluate the degree and direction of GHJ translations in static positions as shown in Figure 9[34]. Many researchers, however, described these methods as having a low reproducibility and diagnostic value in diagnosis [33,34,52]. To improve the diagnostic value, researchers have designed instrumented methods to quantify GHJ translations to detect glenohumeral joint instability with laxity tests [34,53,54,55,56,57,58] The low accuracy of glenohumeral joint instability classification is probably caused by the low accuracy of manual tests to detect glenohumeral joint instability.

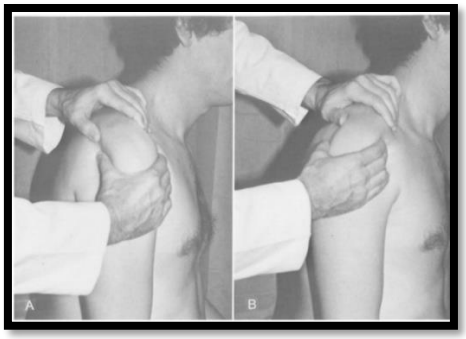

Figure 9. Clinical test to measure glenohumeral laxity [34]

The challenge of biomechanical assessment for this condition is to have reliable quantitative information of the physiological function of the GHJ to detect pathological motion patterns. The differentiation between pathological and healthy kinematic motion patterns can help understand the causality of glenohumeral joint instability.

Of all the surgical procedures, the diagnostic arthroscopy is the most common glenohumeral intrusive intervention [59,60]. Diagnostic arthroscopy has been described to be a gold standard to evaluate glenohumeral instability [59]. Arthroscopy is described as a minimal invasive technique in which an examination and sometimes treatment that is performed using an arthroscope, or an endoscope to do small holes or portals in the skin.

An ideal diagnostic procedure can be applied to a larger proportion of population than arthroscopy without a risk of tissue damage. Arthroscopy can also be applied to repair tissue in surgical procedures and is called arthroscopy treatment. The arthroscopy treatments are reported to have failure rates of 4% to 22% for patients under the age of 30, in contrast physical therapy that has been reported to have recurrence rates of 17 to 96% [61]. The risks of diagnosis arthroscopy and arthroscopy treatment are similar. Even though, arthroscopy has higher success rates than therapy, not everyone can be a candidate to an arthroscopy due to risk factors (high arterial pressure, diabetes, overweight, heart disease). Therefore,

patients older than 50, are less probable to be candidates for diagnostic and treatment with arthroscopy. The population that can be candidate for the surgical procedure can have risk of infection and other risks associated with surgical procedures [62]. Therefore, the use of non-intrusive methods to diagnose glenohumeral instability is a key activity to increase the amount of population that can be diagnosed accurately.

3.2.3 **Biomechanical assessment**

The biomechanical assessment is an essential process in the clinical diagnosis that consists in evaluating the motion patterns of healthy and pathological subjects. The biomechanical assessment provides a quantitative parameter to improve classification and therefore improves the probability of success in intervention as shown in

Figure 8.The biomechanics assessment for glenohumeral joint instability requires kinematic and dynamic data recorded during a motion performed by the subject.

3.2.3.1 **GHJ joint kinematics**

The biomechanics assessment requires kinematics and dynamics analysis that requires to define the degrees of freedom of the GHJ. The GHJ can be fully simulated with 6 Degrees of Freedom (DOF) that can be represented like a ball and socket joint combined with 3 independent perpendicular sliding joints, as shown in Figure 10.

The joint coordinate systems (JCS) are essential to measure joint kinematics. The JCS are cartesian coordinate systems that are embedded in two adjacent body segments. The axes are defined based on anatomical landmarks. As described in [63] , the origin of the cartesian coordinate systems is the "point of reference for the linear translation occurring in the joint, at its initial neutral position". Secondly, the JCS is established based on two cartesian coordinate systems. Two of the JCS are fixed in every body of the joint, and one is "floating"[63]. The GHJ physiological motion require the JCS are computed calculating the 6 DOF between two reference systems placed on the humerus and on the scapula, represented in Figure 11.

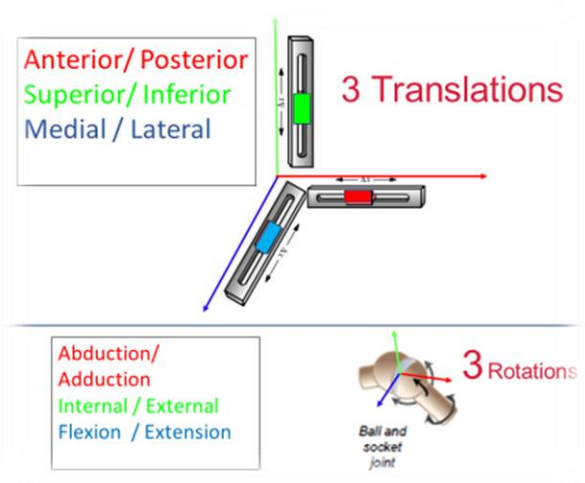

Figure 10. Kinematics of the glenohumeral joint

In a 3D space the GHJ has 3 translations and 3 rotations. Some researchers simplify the GHJ to a 3DOF a ball and socket joint, which has been widely accepted based on the assumption that glenohumeral joint translations (glenohumeral joint translations) were measured with non-accurate methods to be below 1 [mm] [64,65]. Nevertheless, this approach does not consider that subjects can have glenohumeral translations higher than 1[mm] [65]. Recent research has shown that glenohumeral translation can be higher than 1 [mm] [66]. Another limitation in current research is that the glenohumeral joint translations have not been normalized to subject's size and morphology mass and height of each subject.

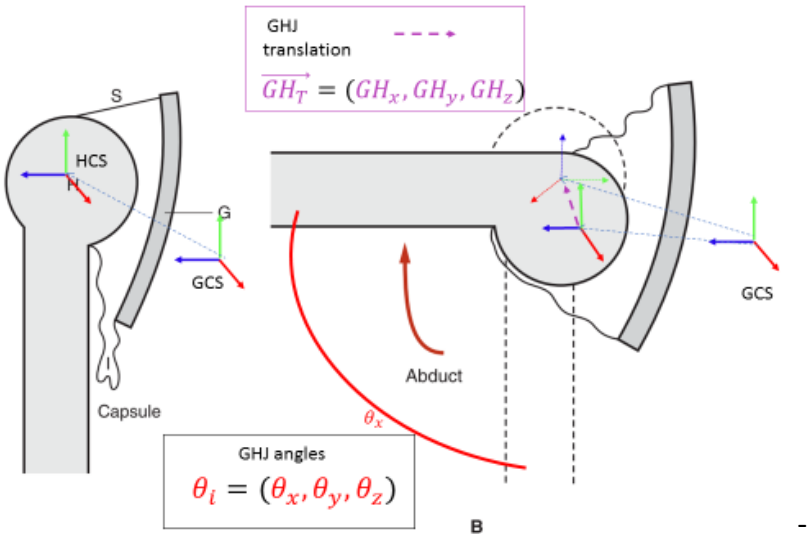

Figure 11. Humerus Coordinate system (HCS) and Glenoid coordinate system (GCS)

In Figure 11 coordinate systems are represented as glenoid coordinate system (GCS) and humerus coordinate system (HCS), which have 3 rotations θ_i and 3 translations $\overrightarrow{GH_T}$. The Figure 11 represents a 90-degree rotation in the "x" axis which brings along a displacement.

Figure 12 represents the coordinate systems that need to be computed from scapula, humerus and thorax. The joint coordinate systems are necessary to measure the joint kinematics of glenohumeral, scapulothoracic and thoracohumeral joints.

The International society of Biomechanics (ISB), gathered researchers in shoulder biomechanics to define conventions to express the JCS of the upper limbs and the shoulder[67]. The coordinate systems are embedded in each bone and are computed to define joint coordinate systems (JCS). The conventions help researchers to compare results and to have the same mathematical language to express joint kinematics.

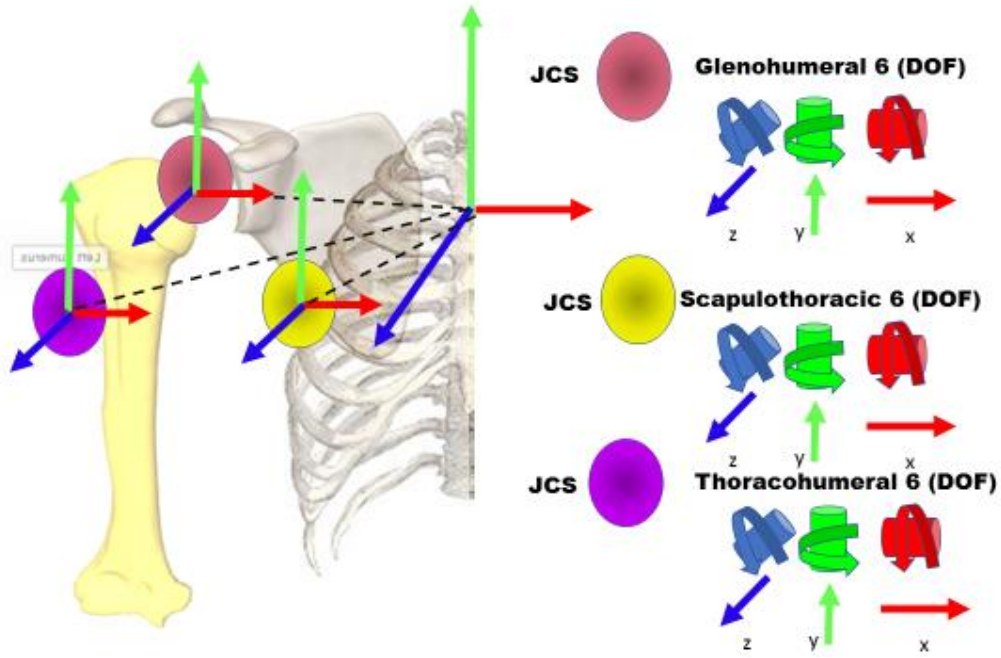

Figure 12. JCS for glenohumeral, scapulothoracic and thoracohumeral 6DOF joints

Each joint has algorithms to compute the DOF that describe motion. The ISB recommends 2 methods to estimate the GHJ centre [68,69], but describes them as non-accurate. Therefore, the ISB recommends the use of medical images to improve the accuracy of the GHJ kinematics [67].

3.2.3.2 **GHJ dynamics**

Dynamics is the area of mechanics that study the cause- effect of motion and the resultant forces and moments. The dynamics of the glenohumeral joint relies on the motion of all the joints and the muscles of all the shoulder joint. In the clinical current practices, the glenohumeral joint instability motion Is assessed mostly with kinematics tests. Nevertheless, researches have also measured maximum isometric muscle force to improve the estimation of the net force that is applied in static positions and during motion[70]. Maximum isometric muscle force is evaluated to create a subject specific evaluation of the force during motion. The maximum isometric muscle forces are used to calculate the forces that are applied in the shoulder joint. However, the dynamic variables that are necessary to detect glenohumeral joint instability are the direction and the magnitude of the internal forces. The Internal forces could only be accurately measured directly In-vivo with intrusive methods or with cadaveric subjects. In the next sections the instrumented methods to evaluate the kinematics and dynamics of the glenohumeral joint instability will be explained. The instrumented methods to evaluate glenohumeral joint instability provide quantitative kinematic and dynamic data that is essential to differentiate between healthy and pathological subjects.

3.3 **Instrumented methods for assessment of glenohumeral joint instability**

The glenohumeral joint is difficult to access directly and palpate, because the glenoid is covered by hard and soft tissue. Medical doctors' clinical current practices evaluate glenohumeral joint instability through medical history, manual tests, medical imaging, and surgical procedures [71]. Researchers have designed methods to assess glenohumeral joint instability that can be classified as: in-vitro and in-vivo and can be subdivided as intrusive and non-intrusive Researchers have used: motion capture systems, medical imaging, musculoskeletal modelling, and other methods to assess glenohumeral joint instability. Previous research has focused on studying glenohumeral laxity with a high accuracy and great progress has been made [52,72]. Non-intrusive instrumented methods have only been validated with cadaveric subjects with gold standard intrusive methods, nevertheless, the non-intrusive methods have not been validated during motion in vivo. Therefore, the instrumental methods measured with cadaveric subjects are not applicable in a clinical context for glenohumeral joint instability diagnosis and classification.

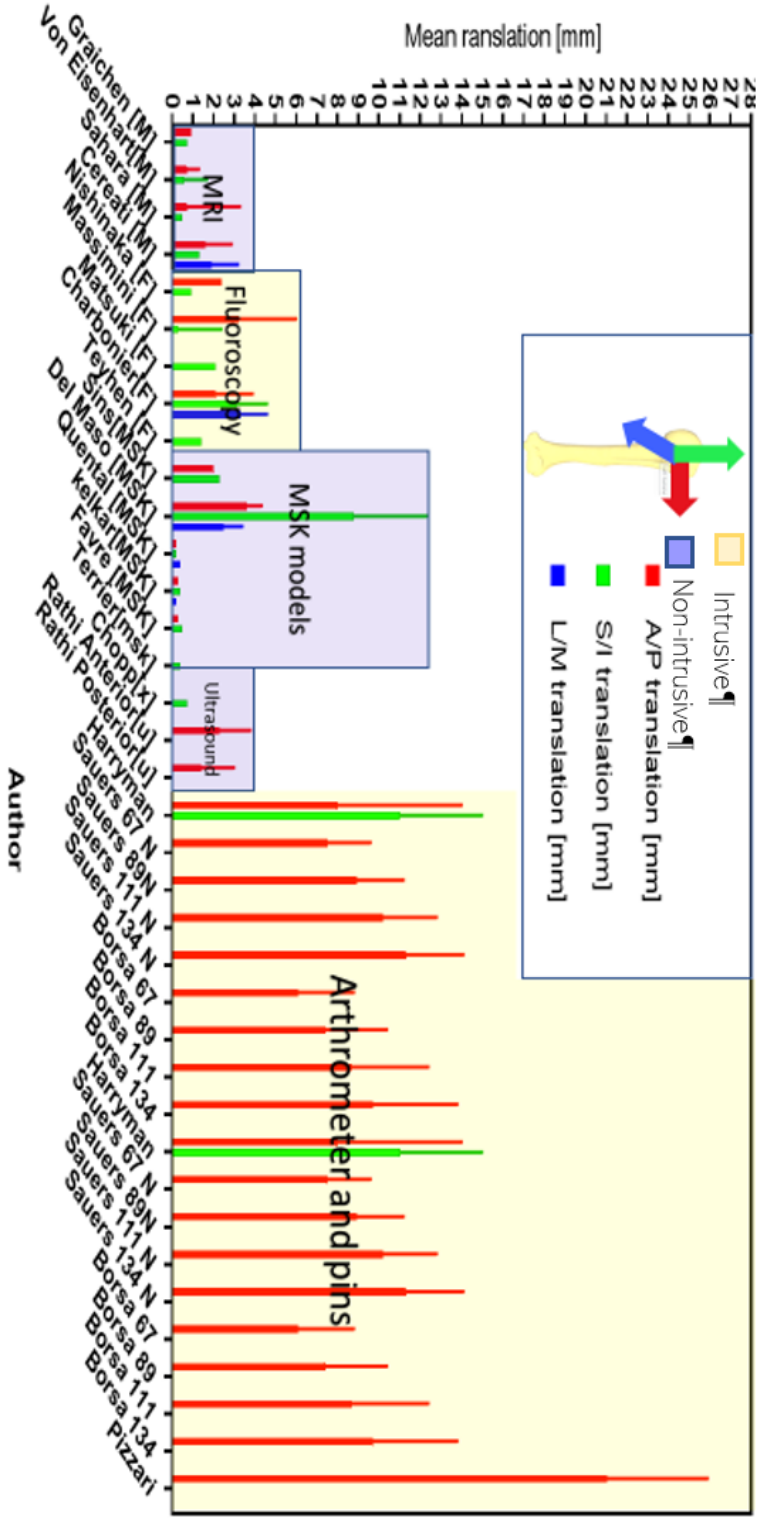

Figure 13. Measurements in glenohumeral joint translations MRI (magnetic resonance Image), MSK(Musculoskeletal) models

The most accurate methods to evaluate the joint kinematics are intrusive. In Figure 13 I compiled 37 measurements of GHJ translations from these the non-intrusive methods are: MRI and MSK models.

Figure 14 shows the most accurate methods to evaluate glenohumeral joint translations during motion and in static positions. The intrusive methods are fluoroscopy, arthrometer and pins. Fluoroscopy has been reported to have absolute measurement errors lower than 0.53[mm] [73]. The non-Intrusive methods: MRI, MSK models and ultrasound have measurement errors>0.33 [mm][40]. The most accurate method to evaluate glenohumeral joint translations during motion is the use of intracortical pins, nevertheless it is a risky and painful surgical procedure that changes the kinematic patterns of healthy subjects due to the pain that is caused.

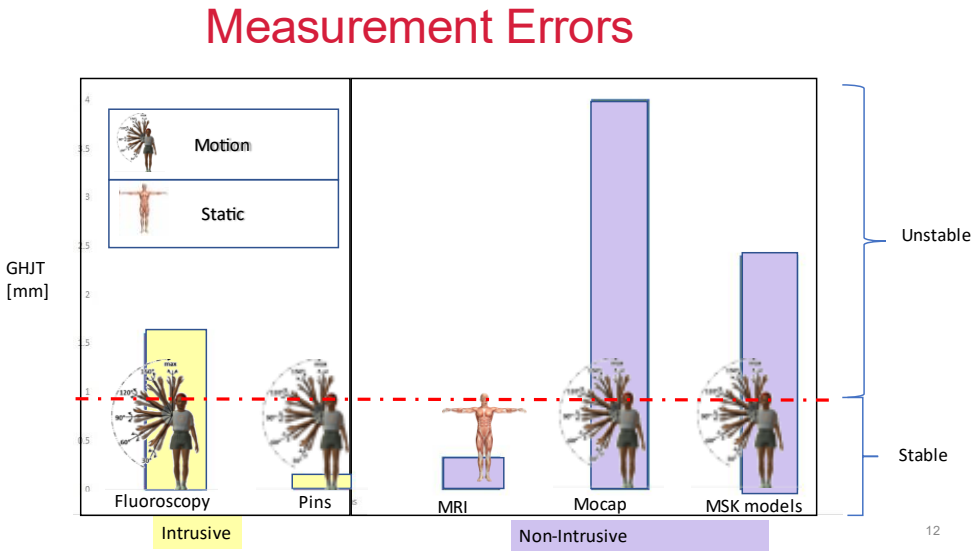

Figure 14 Absolute measurement errors to assess glenohumeral joint translations

Only if non-intrusive measurement errors decrease can the non-intrusive methods replace intrusive methods [74]. In existing research, the errors in non-intrusive methods are significantly larger than the differences between healthy and pathological GHJ [75]. Therefore, if the measurement error is higher than the differences stable and unstable GHJ, then the measurement can lead to an incorrect differentiation between stable and unstable GHJ.

The motion capture systems measure the motion of the human body with the use of sensors, cameras and devices that measure the linear and rotational kinematics. Nevertheless, the motion capture systems have not been accurate enough to measure GHJ Kinematics, but they are essential to estimate scapular rhythm to evaluate GHJ stability and range of motion. Therefore, the data obtained with motion capture systems require to be computed with musculoskeletal software algorithms to estimate simultaneously joint kinematics and internal loading.

Figure 14 shows the measurement error of glenohumeral joint translations and the range of stable and unstable joints. No current non-intrusive method is accurate enough to detect differences between stable and unstable joints [52]. Researchers are finding methods to fill this gap with non-intrusive methods that can be accurate enough to measure accurately GHJ kinematics and kinetics during motion. The musculoskeletal models are the only non-Intrusive methods to evaluate the GHJ kinematics and kinetics. Nevertheless, the accuracy of the musculoskeletal models has not been enough to estimate accurately the kinematics and kinetics of the glenohumeral joint.

3.3.1 **Magnetic Resonance Image (MRI)**

Magnetic resonance imaging (MRI) has been used to assess glenohumeral instability that produces images which can be used to estimate glenohumeral translation [52] [14] [76]. Glenohumeral translation is the relative distance between the humerus head and the glenoid centre.

Certain authors have described the MRI as a gold standard to evaluate glenohumeral instability by measuring glenohumeral translations in static positions [42,61,76]. In contrast, authors have reported that the measurement of glenohumeral translations of the glenohumeral joint in static positions is not accurate enough to evaluate glenohumeral instability [33,77]. Therefore, further research is necessary to validate MRI as a gold standard to evaluate glenohumeral instability in static positions.

The main contribution of MRI in the clinical context is to detect soft tissue structural damage and improve classification and diagnosis of glenohumeral instability. The limitation of static images of MRI is that it has not been able to quantify instability with the calculation of the glenohumeral translations during motion. The glenohumeral translations in static positions cannot be extrapolated to measure instability during motion [42,78].

Additionally, access to MRI can be difficult in a clinical context for patients worldwide. The World Health Organization (WHO) estimated that in 2008 only 10% of the worldwide population had access to an MRI [79]. Authors have reported that there is one MRI machine for every 5.3±11.6 million persons [80]. In summary, MRI is not accessible for most of the worldwide population. MRI is accurate to evaluate glenohumeral translations or soft tissue damage. If MRI is not accessible, non-intrusive alternative techniques are essential to diagnose patients with glenohumeral instability. If MRI is accessible for a patient, then non-intrusive complementary techniques and methods are necessary to improve the diagnosis of the glenohumeral joint instability during motion. Recently, researchers have also used dynamic MRI, which is a sequence of MRI images that can capture glenohumeral translations during motion [42]. Unfortunately, because of its low accessibility, it was not possible to use dynamic MRI for this project.

3.3.2 **Musculoskeletal models**

Musculoskeletal models are computational tools to estimate the joint kinematics and dynamics from the musculoskeletal system. Musculoskeletal models have been used to evaluate glenohumeral instability based on the estimation of glenohumeral joint contact forces [6,81]. However, the estimated peak joint contact forces in thoracohumeral elevation can vary from one author to another between 420 to 2070 [Newtons] and 43 to 110% of the bodyweight [82]. Therefore, the wide range of peak joint contact forces have been described to be “highly indeterminate” and as such not suitable to estimate glenohumeral joint contact forces [82]. The wide range of variation of peak joint contact forces generated the necessity of measuring the joint contact forces with experimental results. Therefore, authors used intrusive methods to measure directly joint reaction forces with biomodular implants [1]. The researchers that have used modular implants to validate musculoskeletal models, have described them as a gold standard to measure glenohumeral joint reaction forces [82]. Biomodular implants are instrumented prosthesis that replace the humerus head and glenoid in an intrusive surgical procedure. The surgical procedure is only applied for patients that require shoulder replacement. Biomodular implants are the only instruments that can measure directly joint contact forces. Accuracy of methods to evaluate glenohumeral joint instability

The methods to evaluate glenohumeral joint instability need to be accurate enough to differentiate between symptomatic and asymptomatic kinematics patterns. The difference

can be detected evaluating glenohumeral joint kinematics and dynamics during the scapular rhythm tests in thoracohumeral elevation. Pathological subjects are detected when having an uncontrolled motion, in this case in the glenohumeral joint instability. Therefore, the Joint contact forces and joint kinematics are fundamental to evaluate glenohumeral joint instability.

3.4 Advantages and disadvantages of methods to evaluate glenohumeral joint instability

Non- intrusive manual tests have been shown to have a low reproducibility [34], and only intrusive methods are accurate in evaluating GHJ instability. An effective intervention relies of a correct diagnosis of GHJ instability. The correct diagnosis of GHJ requires accurate methods to evaluate GHJ instability. The glenohumeral joint instability and other motion related pathologies require a quantitative assessment of the glenohumeral kinematics and dynamics to assess the patients' condition [30]. Nevertheless, there is a lack of gold standard non-intrusive quantitative methods to assess glenohumeral joint instability during motion. The methods to evaluate glenohumeral instability in static positions have not been proven to be accurate enough, or require validation for various classifications of instability [33,38]. The existing gold-standard intrusive methods to evaluate glenohumeral joint instability during motion have risks of radiation [66], or require surgical procedures that can cause harm to the patient[60]. An ideal biomechanical assessment is quantitative, accurate and non-intrusive.

Therefore, researchers are designing methods to improve the accuracy and reproducibility of non-intrusive methods to replace the current intrusive methods to evaluate GHJ instability [52,66,83]. The estimation of the joint kinematics description and the muscle forces are essential to assess glenohumeral instability. Of all the methods to evaluate glenohumeral instability, methods integrating musculoskeletal modelling are the only in-vivo non-intrusive method that can simultaneously estimate glenohumeral joint kinematics, muscle forces and joint contact forces of the glenohumeral joint.

3.5 Musculoskeletal models for glenohumeral joint instability assessment

In a musculoskeletal (MSK) model, the MSK system is modelled as a multi-body kinematic chain comprised by rigid links [84]. MSK models assume that bones are rigid, and that muscles are simulated with idealised springs, dampers, and masses.

The complexity of the shoulder MSK models is that the muscles are attached to one or more joints, furthermore, all the shoulder joints have multiple degrees of freedom (DOF)[85]. The activation in one muscle can generate torque in one axis, and simultaneously generate undesired torque in other axis and joints. Other muscles compensate this undesired torque, involving the whole shoulder kinetic chain [6]. The complexity of modelling the GHJ during motion is that is necessary to measure the complete shoulder.

3.5.1 Musculoskeletal (MSK) models assumptions and implications

Researchers have used MSK models to assess glenohumeral joint instability with two approaches, measuring 3D GHJ translations or joint contact forces. Both methods require the use of algorithms to simulate the shoulder joint: inverse kinematics, inverse dynamics, and static optimization methods. The methods will be explained in the musculoskeletal software section.

Researchers have compared joint contact forces from MSK models with instrumented prostheses [2]. The main limitation for validation is the lack of in-vivo and non-intrusive methods to measure muscle forces. Therefore, the methods based on musculoskeletal models have been the only suitable way to estimate muscle forces and joint contact forces with living subjects [81]. Current models estimate muscle forces and GHJ contact forces based on experimental data from the shoulder motion, which rely on the features of the MSK model.

Researchers have designed models to evaluate shoulder kinematics and dynamics with different research questions and by consequence, different assumptions and algorithms [6,86,87,88]. Even though most of the MSK models are based on the same concepts, every model has different numerical methods, ranges of motion, and assumptions which lead to different results[89,90]. An ideal MSK model simulates in the most realistic way the physiological joint kinematics and internal forces. The accuracy that is needed to measure glenohumeral joint instability with kinematics analysis requires glenohumeral joint translations absolute errors lower than 1[mm] compared with gold standard methods, for instance, intra-cortical pins [52].

The features that are relevant to assess glenohumeral joint instability are: MSK morphology, tissue mechanical properties, glenohumeral constraints, scapular rhythm algorithms and mathematical conventions to express joint kinematics. These features are fundamental for

quantifying the degree and direction of glenohumeral joint instability with musculoskeletal models. All the features that were mentioned previously are essential, but the mathematical conventions to express joint kinematics can be labelled as secondary. The mathematical conventions used by ISB improve the comparison of glenohumeral joint instability for expressing rotations and translations of the joint kinematics with other researchers worldwide. The use of Euler angles with the ISB recommendations helps to avoid the gimbal lock for thoracohumeral elevation [67]. The gimbal lock is a mathematical singularity that causes the loss of one or more DOF for measuring rotations with Euler angles.

3.5.2 Mechanical properties

The mechanical properties of anatomical structures are fundamental to simulate muscles bones and ligaments. The bones are assumed to be rigid elements. The force generating elements are simulated with virtual muscles and torque generators. Hill muscle model is the most used in MSK modelling, shown in Figure 15. The muscles are simulated with vectors that cross the centroid of a sectional cut for every muscle. The muscles are modelled with two types of mechanical components: active (CE) and passive [91].

These virtual muscles are designed to replicate the origins and insertions of muscles in the human body. The muscle-tendon mechanical properties are peak force, pennation angle, optimal fibre length and tendon slack length that are necessary to simulate the force- velocity relationship of muscles contractions. The mechanical properties are obtained from experiments with corpses [86]. The muscle geometry and mechanical properties are used to calculate moment arms and muscle forces that generate human motion. The passive structures are represented with virtual ligaments, coordinate limit forces, springs, and dampers. The MSK models use numerical methods to solve dynamic equations that estimate the mechanical interaction between anatomical structures.

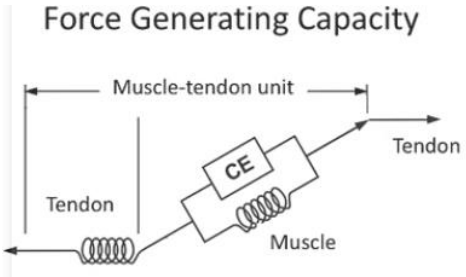

Figure 15. Hill muscle model

3.5.3 Inverse Kinematics

Kinematics describes of how objects move.Figure 16 represents a four rigid bar linked kinematic chain, with a base, and three rotational joints and an end effector in the last segment.

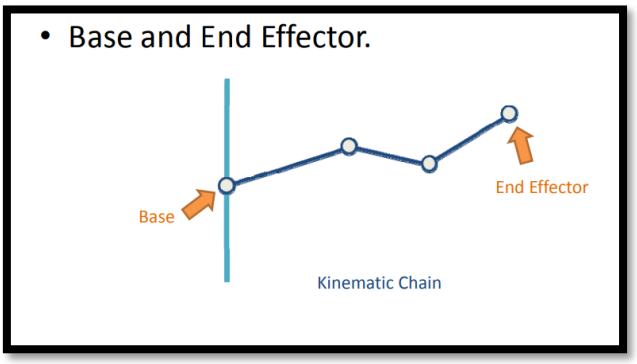

Figure 16. Kinematic chain base and end effector

The goal of inverse kinematics is to compute the vector of joint degrees of freedom $(\theta_1, \theta_2, \theta_3)$ that will allow to localise the point to reach that is represented with a star in Figure 17

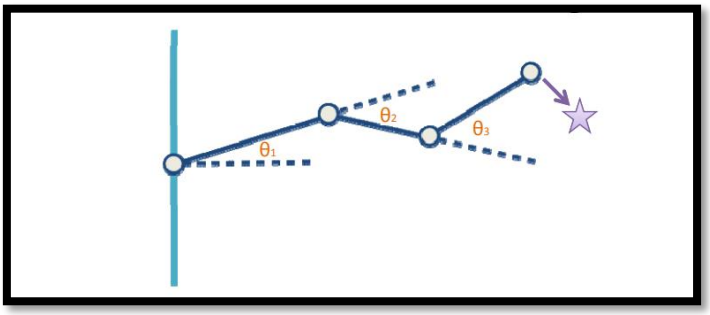

Figure 17. Kinematic chain angles and goal position

For every system, the generalized coordinate can change depending on how the kinematic joint is modelled and the DOF of the system. In Figure 17 the generalized coordinates are the angles between the bars. In musculoskeletal modelling the Inverse kinematics computes the joint angles with the minimal error to estimate the coordinates from the end effector. The goal of inverse kinematics is to estimate the joint angles from cartesian coordinates from anatomical markers. For a musculoskeletal software, the Inverse Kinematics (tool estimates an angle that "best matches" experimental marker coordinate data for every time step.

3.5.4 Inverse dynamics

For the shoulder, the Inverse dynamics is applied to multi-body systems thar are driven and connected by external and internal forces. The inverse dynamics problems are to estimate the internal forces based on the motion and external forces. The inverse dynamics determines the generalized forces that cause motion. The inverse dynamics is based on the classical mechanics principle of the second law of Newton. The Force is dependent to the mass and acceleration; therefore, the inverse dynamics solves the equations of motion to determine all the moments that generate motion. The joint angles that are obtained of the inverse kinematic of the musculoskeletal kinematics and inertial properties are used to calculate the moments based on the external forces that are applied. To solve the equations of motion the dynamic equilibrium conditions and boundary conditions of the musculoskeletal model need to be accomplished [92].

In musculoskeletal models the inverse dynamics require the use of joint kinematics and dynamics to estimate the internal moments[93]. To calculate the moments, it is necessary to know the anthropometric and inertial parameters for each body segment of the musculoskeletal model[94].

3.6 Musculoskeletal models and software

Musculoskeletal software are designed to evaluate the joint kinematics and dynamics of the bones and muscles using equations to simulate the muscles, tendons, ligaments and bones of the human anatomy[95].

3.6.1 Scaling of musculoskeletal model

Scaling is a process to modify the dimensions of the bones of a musculoskeletal model to the size of a specific subject [96]. The localization of the virtual markers that are estimated in the musculoskeletal models need to be as close as possible to the markers that were captured experimentally. The accuracy of the scaling process depends completely Inverse kinematics and Inverse dynamics methods. Therefore, accuracy in scaling is essential to improve the accuracy of a simulation [97].

Measurement-based scaling uses the distance between the virtual markers of the model and the experimental kinematic markers. This method uses scaling factors for every segment in one or more direction [97]. The factors are used to scale the generic model to the size of the

specific subject. The scale is the proportion that the generic model is multiplied to have the size of the specific subject. For example, a scale factor of 2, means that the generic body of the model requires to be two times bigger than the original generic model [98].

3.6.2 Glenohumeral ball and socket and stability constraints

There are two constraints to model the GHJ with this assumption: ball and socket joint and the stability constraint. The ball and socket constrain defines the glenohumeral DOF with three independent rotations. The stability constraint is implemented starting from the assumption that the muscle forces generate a resultant force that is directed to an ellipsoid or circle [99],

Figure 18 GHJ stability is evaluated with the direction of the joint contact forces. The resultant of the joint contact forces in the humerus is directed outside the glenoid this means that the joint is unstable and could lead to a dislocation or subluxation.

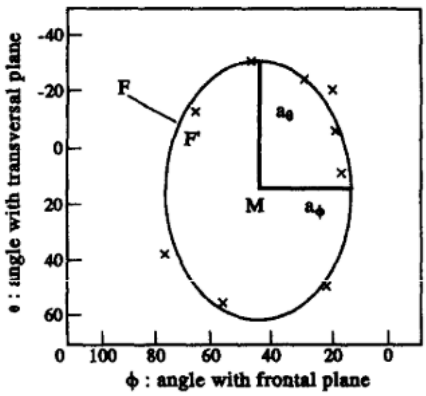

Figure 18.Elipsoidal constraint for GHJ contact forces

Even though, these two constraints are the most used, the limitation of these two constraints is that current musculoskeletal models have not compared both constraints with gold standard methods the accuracy to estimate the joint contact forces with the force stability constraint algorithms. Research has been done to compare the joint reaction forces of another algorithms of a different musculoskeletal model with biomodular implants with an overestimation of joint reaction forces up to 33%[2]. A limitation of simulating the GHJ as a ball and socket joint is that it cannot be compared with direct measurements of GHJ translations that are obtained with experimental methods[72].

3.6.3 Force directed kinematics assumption

Force directed kinematics consists in modelling the joint with 2 more directions glenohumeral joint translations than the ball and socket assumption. The equations are solved assuming a quasi-static equilibrium between the forces generated by GHJ translation and the inertial forces in the humerus and. The force directed kinematic forces are expressed as: (F_{SIS}, F_{SAP}), which are calculated based on the assumption that forces can modify the glenohumeral joint translations. F_{SIS} is the superior inferior force and F_{SAP} is the anterior posterior force. The force directed kinematics assumes that there is a" quasi-static equilibrium between the inertial forces and the force directed kinematics reaction forces in two anatomical planes"[37]: $inferior - superior(F_{SIS})\ and\ anterior - superior(F_{SAP})$ [100], represented in

Figure 19. Dynamic equations are solved for the range of motion that is measured to obtain a kinematically determined system. Muscle forces, JRF, moment arms are calculated simultaneously with joint reaction forces. The dynamics of the muscles changes with GHJ translation because the translations affect the moment arms [37].

The translations are assumed as elastic components that are in dynamic balance with the labrum and the ligaments. The GH ligament is defined by a stress–strain model [100].

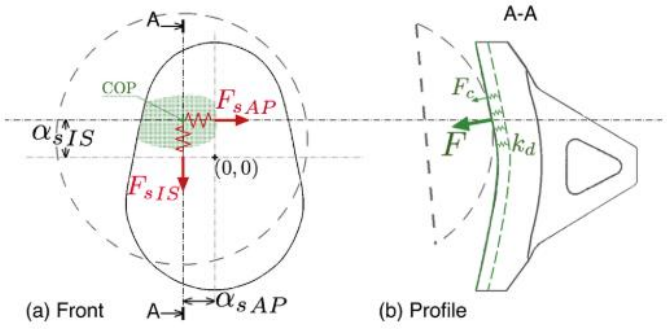

Figure 19. Force dependant kinematics

The advantage of this methods is that it can calculate GHJ translation in motion and be compared with gold standard methods [26,66,101]. Nevertheless, this calculation also relies on numerical methods to simulate the shoulder joint JRF: inverse kinematics, inverse dynamics, and static optimization methods. The numerical methods require validation of

experimental data or to be tested to be used for clinical applications based on recommendations for good practices for musculoskeletal models [102].

3.6.4 Surface Joint Contact Constraint

Another adaptation from the ball and socket model considers the assumption that there is contact between the interfaces of two components of the GHJ. These constraints have only been used by the Anybody model and has been applied to a “nonconforming total shoulder arthroplasty (NCTSA)” [37]. The technique applies 3D models of surfaces that represent the bones. The assumption allows humeral head penetration in the glenoid. This technique has been used with prosthesis that are computed aided designed (CAD) [37]. Further research is required to be implemented with non-surgical shoulders. The surface contact constraint has only been used by the Anybody model that will be described an evaluated in section 7.7.

3.6.5 Scapular rhythm algorithms

Scapular rhythm algorithms are based on the theory that the relationship between the scapular and humeral motions are consistent and dependent [70]. Therefore, researchers have developed statistical models that estimate joint kinematics with skin-marker motion capture experimental data from the shoulder [70,103,104,105]. The next section will compare six out of seven MSK models that use scapular rhythm algorithms and will describe the respective advantages and disadvantages. The scapular rhythm algorithm is essential to evaluate GHJ motion and the interaction with other joints in the shoulder

Six out of seven MSK models that were ranked in this research use scapular rhythm algorithms. One of the applications of scapular rhythm algorithms in musculoskeletal models is to estimate the internal forces by solving the force and momentum equilibrium equations from bone positions to generate a determinate system relative to the reaction for all the bones of the shoulder joint [106]. The scapular rhythm algorithms estimate the scapula and clavicle angles based on the thoracohumeral angles. Therefore, scapular rhythm has been used for the musculoskeletal models to estimate joint kinematics and internal forces of the GHJ.

.

3.6.6 Holzbaur Shoulder Model

The Holzbaur model is designed to estimate tendon -muscle lengths and moment arms to identify shoulder motion patterns to differentiate between groups of subjects. The main applications are cuff tear, surgical procedures, and neuromuscular simulation.

The Holzbaur model uses the scapular rhythm algorithm based on the research of Groot *et al* [70] to interpolate the position of scapula and clavicle based on the humerus position with a linear regression of scapula and clavicle with the kinematics data of humeral motion.

The scapular rhythm algorithm is based on predictive equations that are regression equations that associate the thoracohumeral angle to the scapulothoracic angle during motion. The regression equations do not include a GH stability constraint which could lead to simulate dislocations [107]. Instead, The Holzbaur model use virtual moments and forces in every DOF named Joint Restraint Functions [90], which simulate the function of ligaments and soft tissue. The authors of this model report muscle-tendon properties with Hill type muscles obtained from cadaveric experiments [86]. The limitation of this model is that it lacks validation for estimation of the centre of rotation in the humerus head with gold standard methods for 90 degrees shoulder thoracohumeral elevation.

The anthropometric values are obtained from an average European male. The scapular rhythm was validated for an 30^0thoracohumeral elevation. The creators of the Holzbaur model report differences in angles between 15 to 94% compared with intracortical-pins [108], nevertheless, the authors do not report errors for the full range of shoulder abduction.

Holzbaur model has most of the essential features to assess glenohumeral joint instability. Further research is required validate the glenohumeral constraint to measure GHJ contact forces with experimental glenohumeral angles and glenohumeral joint translations. The GHJ constraints also require to be evaluated for a 90 Degree abduction for healthy participants to be able to evaluate glenohumeral joint instability

3.6.7 **DSEM shoulder model**

The Delft Shoulder and Elbow Model (DSEM) has been used to calculate joint contact forces and joint moments in the shoulder joint [6]. The DSEM model simulates internal forces for different tasks. DSEM has been shown to be helpful for simulating the effects of surgeries for

daily life tasks. DSEM model is created generic anatomical geometries, with a scaling method that fits the size of the subject [6].

The DSEM has been used to calculate moment around the combined axis of rotation of the shoulder joints [6]. DSEM models the muscles as TRUSS (tensile force generating elements) which are finite element with deformation nodes [6]. The TRUSS is expressed as a function of displacement between nodes. The ligaments are modelled as passive rigid elements which can only be loaded in tension. The GHJ contact forces are estimated using a ball and socket and a stability constraint. The disadvantage of this approach is that it models the muscle forces to be centred in the GHJ. The opposite of this happens in the shoulder, in reality- the GHJ is centred by the muscle forces.

DSEM model have compared with an instrumented shoulder endoprosthesis [2]. For this research, electromyography-signals optoelectronic motion data, external forces, and in-vivo GHJ reaction forces (GHJRF) were measured for two patients with a modular implant, during dynamic tasks [2]. The MSK model is reported to overestimate the GHJ contact force (glenohumeral joint contact forces) 34% compared to the modular implant, and reduced to 23% or relative error with an energy cost function [109]. Another study evaluated the DSEM model with intra-cortical pins with 10 to 29% of difference to evaluate GHJRF [110].

This model neglects glenohumeral joint translations, this could be the cause of the overestimation of JRF compared with the direct force measurements with bio-modular implants. Angles are expressed with XYX Euler angles for joints relative to the sternum. Which were adapted to match the ISB recommendations, which are helpful to measure joint kinematics and compare with other researchers results.

Another limitation from this model is that it does not include algorithms for scapular rhythm. Therefore, this model cannot estimate the ratio of glenohumeral angles with scapulothoracic angles and thoracohumeral rotations. The scapular rhythm is a feature that will need to be included and evaluated in this model to improve the glenohumeral joint instability assessment. The accessibility of the DSEM models permits the use of open-source software to adapt the numerical methods for different research questions. Nevertheless, the software is not fully accessible for glenohumeral stability.

3.6.8 **AnyBody Shoulder model**

AnyBody is an MSM model named after a commercial musculoskeletal software that simulates motion from living beings. The Anybody shoulder model has been used to evaluate the effects of the muscles, medical implants, and wheelchair propulsion with an MSK shoulder model. The anthropometric values are the same as the Holzbaur model. The constraints for the GHJ are the same that in the DSEM model and the scapular rhythm kinematics linear regression were adapted from the Holzbaur model [108,111]. The difference is that this model is derivative on Bergmann et al, which measured reaction forces in the GHJ during arm abduction [1], with underestimates the GHJRF 12% compared with direct measurements from modular implants [82]. The Anybody model underestimated the value of the GHJ contact forces probably caused by the morphological and kinematic differences between healthy subjects and patients with total shoulder replacement [36].

Sins defined 2 different glenohumeral constraints that can be implemented in this research [112] [37], forced directed kinematics and surface contact constraints, which require to be tested with experimental motion data to evaluate the accuracy to measure GHJ translations.

The disadvantage of the current publications with the Anybody model is, that it has not been validated directly for GHJ scapular kinematics with gold standard methods. The validation could be done with the use of direct measurement of GHJ translations with arthroscopy or with medical images. Same as other models, this model can have computational errors generated by the incorrect estimation of joint kinematics and internal forces that could be solved improving the algorithms to detect the GHJ kinematics.

3.6.9 **Wu model**

The Wu model is a 5 segmented musculoskeletal model with 10 degrees of freedom of the upper limb that was developed in OpenSim. The model was originally designed for inverse kinematics and dynamics. The glenohumeral and acromioclavicular joint were modelled as ball and socket joints. The sternoclavicular joint was modelled with 2 rotation degrees of freedom. The model is comprised by 26 Hill-type muscle tendon units. The muscles represent the “axioscapular, axiohumeral and scapulohumeral” muscle groups [113]. Muscle paths were determined with optimal wrapping via points locations based in the anatomy of the visible human male [87], the model was adapted to fit moment arms that were measured with 8 cadaveric subjects [114]. The scaling of the moment arms was adapted to the anthropometry

to the 8 subjects. The Wu model allows to scale the musculotendon lengths, inertial properties, and moment arms to the distance of the bony landmarks [115]. The Wu model fits exactly the ISB recommendations to express joint kinematics and dynamics.

3.6.10 **Ranking of MSK shoulder models**

Eighteen shoulder musculoskeletal models were found in the literature. Among these, all of which simulated the glenohumeral with at least 3 degrees of freedom were chosen to be evaluated. To detect the existing models that can assess glenohumeral instability, eighteen features were evaluated in 9 available shoulder musculoskeletal models that can evaluate glenohumeral kinematics and dynamics, shown in Table 1. After evaluating the eighteen features, two models were chosen to study joint kinematics and dynamics. All the models that are described in Table 1 have two different algorithms that are used to evaluate glenohumeral stability. The algorithms that have been used are shoulder rhythm and the glenohumeral joint

constraint algorithm. Shoulder rhythm is designed to detect the position of scapula based of the position of the humerus relative to the thorax. The glenohumeral joint constraint algorithms define the degrees of freedom and the relationships between the joint kinematics and the glenohumeral joint reaction forces.

Model	Essential features									Complementary features								
	GHJ Constraints			SR algorithm			Muscle-tendon Mechanical properties			MSK morphology parameters			Ligament mechanical properties			ISB Kinematic conventions		
	Validation	Full Description	Availability	Validation	Full Description	Availability	Validation	Full Description	Availability	Validation	Full Description	Availability	Validation	Full Description	Availability	Validation	Full Description	Availability
1. Holzbaur			■		■	■		■	■		■	■			■		■	■
2. Wu			■			■		■	■		■	■		■	■	■	■	■
3.DSEM	■	■			■			■	■		■	■		■	■			
4.Anybody		■		■				■	■		■		■	■	■		■	■
5.Swedish	■			■	■					■	■	■					■	
6.Dickerson		■	■		■			■		■	■	■						
7.Newcastle		■			■					■	■	■				■	■	■
8.Garner							■	■	■	■	■	■				■	■	■

Table 1. Musculoskeletal models to evaluate Glenohumeral instability.

The models were ranked by three different criteria: validation, full description, and availability. The models that have full description in the scientific paper explain how to replicate the model and can help understand the equations and definition of the assumptions of the model. The criteria to accept the validation of the feature describes if the authors validated the model´s outcome with a gold standard method. In addition, the availability of the musculoskeletal model is defined by the accessibility to the software and the methods to

use the model to estimate the glenohumeral joint kinematics and dynamics. Therefore, after reading the scientific articles and exploring the musculoskeletal models, two models that have the highest rank based on the features and the accessibility to the model: Holzbaur and Wu model.

The features of Table 1 are selected based on the sensitivity of the features to improve the estimation of the glenohumeral joint reaction forces. For instance, the glenohumeral joint constraints have more influence over the joint reaction forces than the other features. Therefore, to choose the best models three characteristics were considered. Full description, validation, and availability. These three characteristics are based on previous literature[102], to improve the replication of the results of the estimation done by other authors The Holzbaur and Wu model have the most important features with the most important characteristics. Furthermore, both models have the minimal degrees of freedom and constraints to estimate joint reaction forces, which are reported to be essential to improve the diagnosis of GHJ instability,

The Wu model was chosen over the DSEM model because it is directly expressed with the international society of biomechanics conventions. The international society of biomechanics created conventions to express kinematics to improve the communication between researchers unifying the language to express joint kinematics. The Holzbaur[86] model and the Wu model[115] have the most important algorithms that are used in all the models that were evaluated in the

Table 2. Therefore, the comparison of the two models will be oriented to understand the differences between outputs of the two most important assumptions that are used in the literature: Scapular rhythm algorithm, and glenohumeral joint stability constraint.

4 METHODS

4.1 Motion capture process

Kinematic data was obtained with a BTS SmartDX optoelectronic motion capture system comprised by eleven infrared cameras that captured cartesian coordinates of skin reflective markets of the shoulder joint with a frequency of 250 frames per second. The participants did three cycles of shoulder elevation following a metronome with twenty beats per second.

Every participant signed an informed consent approved by the ethical committee of the biomechanics lab of the Mexican Neurobiology institute. We requested the participants to do a 90-degree thoracohumeral elevation in 3 seconds in the first sound of the metronome. The subject sustained the thoracohumeral elevation for 3 seconds from between to beats of the metronome, and other 3 seconds for the thoracohumeral return to the neutral position.

4.1.1 Marker placement

The BTS Bioengineering SmartDX optoelectronic motion capture system was used to obtain 3D Cartesian coordinates of 16 photo-reflective markers that were placed in anatomical landmarks that are visualized in

Figure 20 and Figure 21. The reflective skin markers were placed based on the markers in OpenSim of the Wu Model without including the centre of humerus head and elbow centre [115]. The kinematic data was obtained with a 250 [Hz] sample rate. The 3D cartesian coordinates of markers were filtered with an 8 Hz Butterworth low pass filter with 1.10 Smart Analyzer. Data was also smoothed with a triangular function in Smart Analyzer software from BTS Bioengineering.

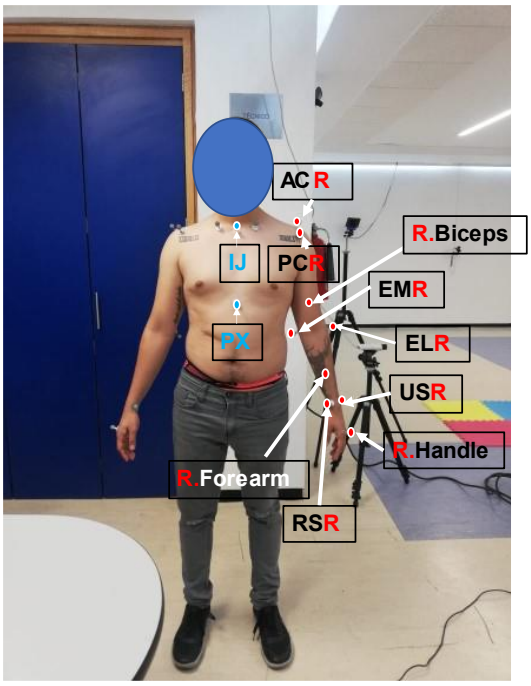

IJ Incisa Jugularis
PX Processus Xiphoideus
PCR,Processus Coraceiodeus. The most ventral point of processus coracoideus.
EMR. (Medial Epycondile) Most caudal point of medial epycondile
ELR.(Lateral Epycondile) Most caudal point of lateral epycondile
RSR: (Radial styloid)Most caudal- lateral point of radial styloid
USR (Ulnar Styloid) Most caudal- medial point of ulnar styloid
R.Biceps. Half distance between **PC** and **(EL+EM)/2**
ACR The most dorsal point of acromioclavicular joint
R.Forearm. Middle point between **RS** and **EL**

Figure 20 Marker placement shoulder motion capture. Anterior view

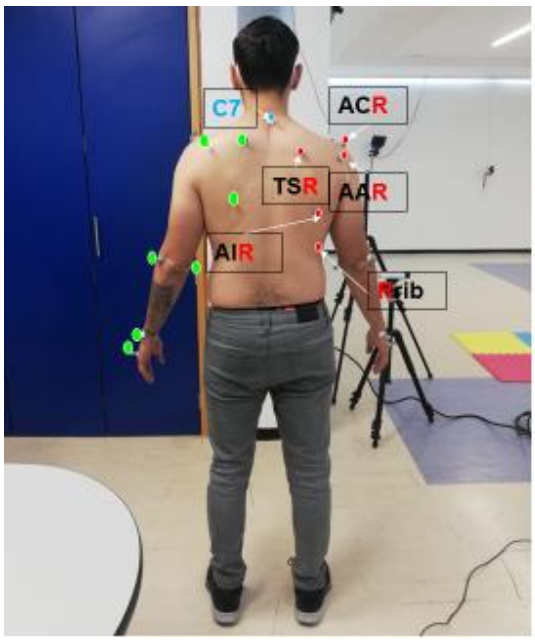

TS. Trigonum scapulae, In the medial border of the medial scapula and aligned with scapular spine

AA, Angulus acromialis. In the dorsolateral curvature of the scapular spine

AI, Angulus iIncisa Jugularis. The most caudal point of the scapula.

AC, The most dorsal point of the acromioclavicular joint.
C7. The most pronounced point in C7

Rrib. Lowest point in False right rib 10

Figure 21 Marker placement shoulder motion capture. Posterior view

The kinematic model was exported to be evaluated with 2 models: Holzbaur [116] model in OpenSim (version 3.3, Stanford University, Stanford, CA), and Wu Model in OpenSim (version 3.3, Stanford University, Stanford, CA)[113].

4.2 Kinematic model development

The kinematics of the two shoulder models that are compared are comprised by three joints to simulate the shoulder joint. The musculoskeletal models simplify the shoulder to three ball and socket joints: glenohumeral, sternoclavicular and acromioclavicular. The International Society of Biomechanics (ISB) conventions were used to express the nine rotational degrees of freedom that are expressed with different references systems for every degree of freedom

Figure 22.

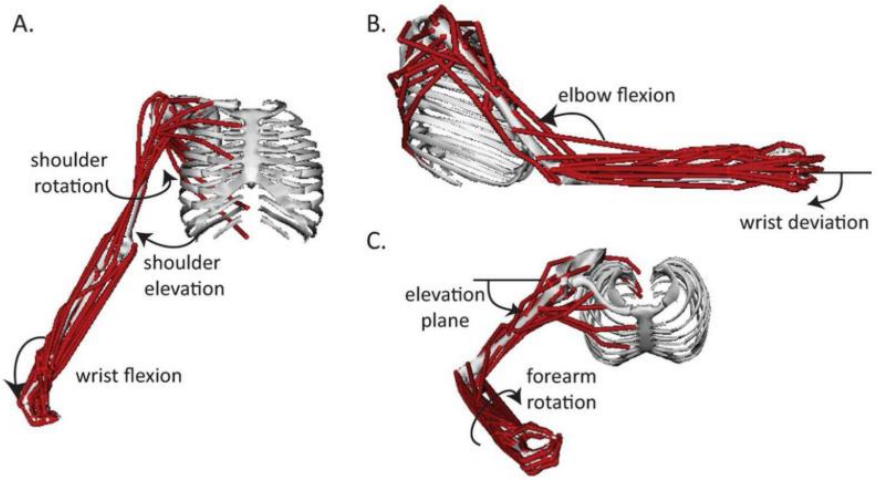

Figure 22.Shoulder and elbow rotations

4.2.1 Range of motion and degrees of freedom

For the three models that were chosen, the range of motion of the shoulder joints is evaluated based on the conventions that have been proposed by the International Society of biomechanics (ISB)[67].

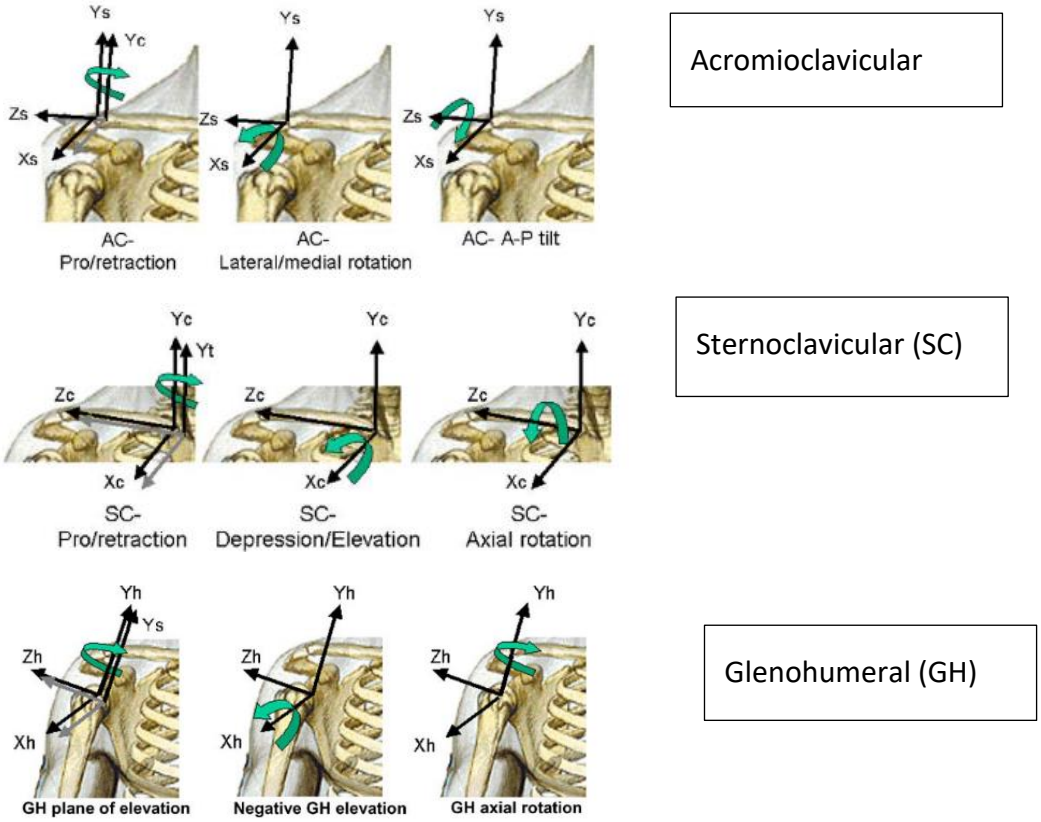

Figure 23. Acromioclavicular, sternoclavicular and glenohumeral joint coordinate system (JCS) and degrees of freedom [67]

The joint coordinate systems (JCS) of the acromioclavicular, sternoclavicular and glenohumeral joint that are shown in

Figure 23 are conventions that are used to express the degrees of freedom of the joints. The JCS define the angles of the bones in a 3D space for every joint. The glenohumeral, acromioclavicular and sternoclavicular joints rotations are defined in

Table 2.

Convention	GHJ DOF	GHJ Mathematical language	Acromioclavicular	Sternoclavicular joint DOF	Software
ISB	(Ys) Plane of elevation	Euler YZY´	(Y+) Protraction -Retraction	(Y+) Protraction -Retraction	OpenSim
	(Yh) Axial rotation		(Z +) Posterior tilt -Anterior tilt	(Z+) Posterior -depression	
	(X)Elevation		(X+) Medial rotation -Lateral rotation	(X+) Depression -Elevation	

Table 2.Degrees of freedom and coordinate system for 3 MSK models (recheck)

4.2.2 Coordinate transformation from Holzbaur to ISB recommendations

The Holzbaur model has similar conventions to express rotations than ISB, but the mathematical language has differences that have been described in

Figure 24 [117]. The main differences are that the Holzbaur model is expressed in spherical coordinates and the ISB recommendations are expressed in Euler angles. Therefore, to express the Holzbaur in the same mathematical language than the ISB recommendations [67] in order to compare the Holzbaur model to other models, it is necessary to use the same mathematical language and conventions that are proposed by the ISB. Therefore, the Holzbaur model requires to be transformed to the ISB recommendations conventions [67].

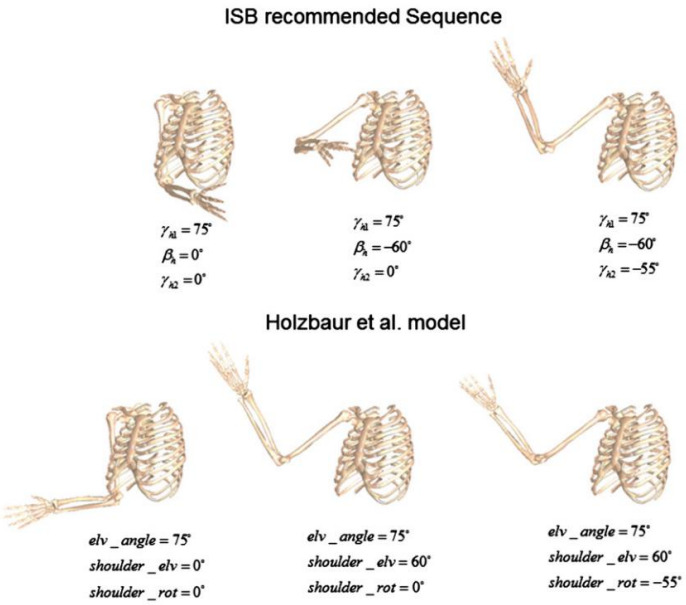

Figure 24 Differences between the ISB recommendations and the holzbaur model [118]

The rotations between the Holzbaur model and the ISB conventions are expressed in Equation 1. Where $\left[t(p)R^{h(R_{ISB})}\right]$ is the matrix that changes from the Holzbaur model to the ISB recommendations expressed in Euler angles YXY. The Euler angles are expressed as: $(\boldsymbol{\gamma_{h1}}, \boldsymbol{\beta_h}, \boldsymbol{\gamma_{h1}})$ and $t(p)R^{h(R_{ISB})}$ is the matrix to transform from the Holzbaur degrees of freedom in spherical coordinates to the ISB recommendations coordinates in Euler angles.

$$\left[\boldsymbol{t(p)R^{h(R_{ISB})}}\right]\left(\boldsymbol{elv_{angle}}, \boldsymbol{shoulder_{elv}}, \boldsymbol{shoulder_{rot}}\right) = [\boldsymbol{R_{YXY}}]\ (\boldsymbol{\gamma_{h1}}, \boldsymbol{\beta_h}, \boldsymbol{\gamma_{h1}}) \qquad \textbf{Equation 1}$$

In the matrix $[R_{YXY}]$, following the ISB recommendations [67], the angles are extracted with the following equations:

$$\left[t(p)R^{h(R_{ISB})}(\gamma_{h1}, \beta_h, \gamma_{h1})\right] = \begin{bmatrix} t_{11} & t_{12} & t_{13} \\ t_{21} & t_{22} & t_{23} \\ t_{31} & t_{32} & t_{33} \end{bmatrix} \ldots\ldots\ldots..equation\ 2$$

$$= \begin{bmatrix} cos\gamma_{h1}cos\gamma_{h1} - cos\beta_h sin\gamma_{h1} sin\gamma_{h1} & sin\gamma_{h1}sin\beta_h & cos\,\beta_h\, cos\gamma_{h1}sin\gamma_{h1} + cos\gamma_{h1}sin\gamma_{h1} \\ sin\beta_h sin\gamma_{h1} & cos\beta_h & -cos\gamma_{h1}sin\beta_h \\ -cos\,\gamma_{h1}sin\gamma_{h1} - cos\gamma_{h1}cos\beta_h sin\gamma_{h1} & cos\gamma_{h1}sin\ \beta_h & cos\gamma_{h1}cos\beta_h cos\gamma_{h1} - sin\gamma_{h1}sin\gamma_{h1} \end{bmatrix}$$

from which:

γ_{h1} =arctan2(t_{12}, t_{32}) ..... Equation 3.a

γ_{h2} =arctan2(t_{21}, t_{23}) $if\ \gamma_{h2} < 0\ \rightarrow\ \gamma_{h2}$=arctan2$(t_{21}, t_{23}) + 360$.....Equation 3.b

$$\beta_h = \arccos\,(t_{22})\text{.....Equation 3.c}$$

The Holzbaur model is described with spherical coordinates, to compare both models the Holzbaur model requires to be transformed to YXY Euler angles. The equations 3.a, 3.b and 3.c have as an output the Euler angles of the Holzbaur model expressed in the ISB recommendations[63]. The advantage of expressing all the models with the same conventions is that the differences between the algorithm outputs can be evaluated.

4.2.3 Musculoskeletal models workflow in OpenSim

Of the musculoskeletal software, OpenSIm has the advantage of having opensource, available and full description of the algorithms that are used to estimate the joint kinematics.

The musculoskeletal generic models in OpenSim requires four steps to evaluate glenohumeral joint contact forces in the OpenSim software: Inverse kinematics, inverse dynamics, static optimization, and joint reaction forces analysis. Every step is computed with algorithms to estimate joint angles, joint moments, muscle forces and joint forces[102].

Figure 25 shows the four algorithms that are necessary to estimate joint contact forces.

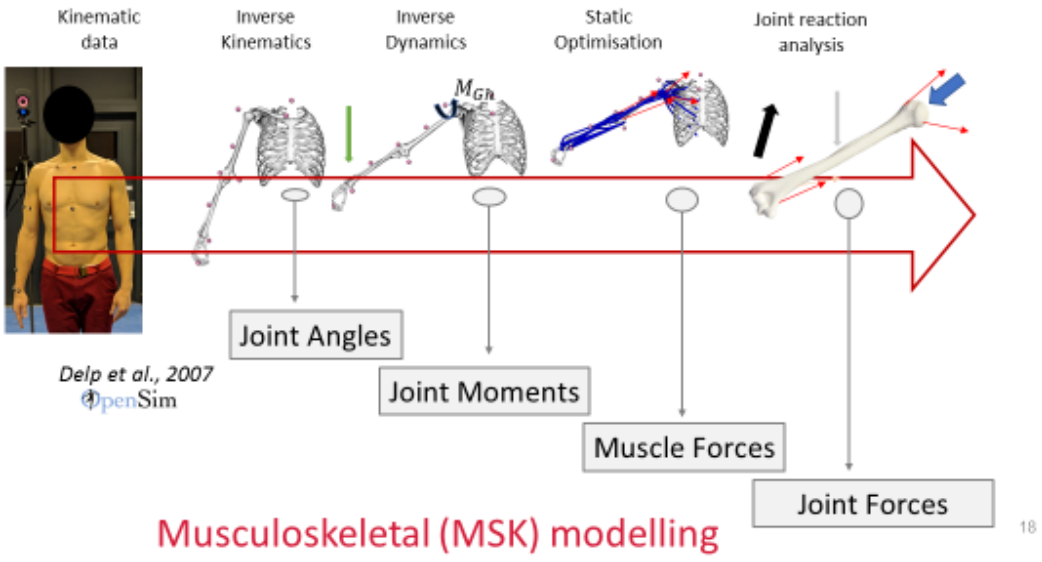

Figure 25. Shoulder Musculoskeletal models workflow

The existing shoulder models have evaluated glenohumeral joint instability with the estimation of the direction of the joint reaction forces of the scapula and humerus or with glenohumeral translations. The glenohumeral joint contact forces have been compared with biomodular implants obtained from experimental data from patients with total shoulder

replacement [36]. Nevertheless, the joint contact forces have not been compared with different musculoskeletal models with the same input (experimental kinematic data). Therefore, it is important to compare the estimation of internal forces of the existing musculoskeletal models to quantify the differences between different algorithms and methods to understand the cause-effect relationships between the kinematic experimental data and the estimation of the inverse kinematics and joint contact forces. The comparison of the existing models that estimate joint contact forces with musculoskeletal models is a first step to evaluate the accuracy of musculoskeletal models' algorithms to evaluate glenohumeral joint instability. Therefore, the accuracy of joint kinematics and inverse dynamics are fundamental to calculate joint contact forces.

The existing quantitative methods estimate the direction of instability during motion to assess glenohumeral instability. There are two approaches to evaluate glenohumeral instability. In the first, it is measured with glenohumeral translations assuming a 6 degree of freedom joint. In the second, estimating the direction of the glenohumeral joint contact forces, neglecting the glenohumeral translations and assuming that the glenohumeral joint is a 3 degree of freedom ball and socket joint [6,87,119,120]. In this second assumption, the criteria to detect glenohumeral instability is evaluated with the direction of the net joint reaction forces of the humerus during motion[6]. Both methods require the estimation of the glenohumeral joint reaction forces to estimate the direction of the forces or the glenohumeral joint translations. The joint reaction forces of both methods depend on the accuracy of the estimation of the inverse kinematics and inverse dynamics. In this research both models that will be compared assume the glenohumeral joint as a ball and socket. Therefore, no glenohumeral translations will be considered. The accuracy of the calculation of the joint reaction forces depends on the morphology of any musculoskeletal model. If the models replicate accurately the morphology of the subject, then the accuracy of the estimation of the joint reaction forces will be higher. Therefore, the accuracy of the location of the muscle attachments is essential to improve the accuracy of the calculation of the muscle forces and the joint reaction forces.

4.2.4 **Inverse kinematics implementation**

The inverse kinematics algorithm is designed to estimate the values for every degree of freedom that "best match" the trajectory of the experimental markers coordinates [121].

The inverse kinematics process was performed using the OPENSIM software. The algorithm was implemented with a global optimisation approach using the equation 4. $\vec{x}_i^{exp}$ (The

experimental markers obtained with the motion capture system) and the markers of the MSK model $\vec{x}_i(\vec{q})$.

$$\min_{\vec{q}} \sum_{i=1}^{M} w_i \left\| \vec{x}_i^{exp} - \vec{x}_i(\vec{q}) \right\|^2 \qquad \text{Equation 4}$$

The angles were computed using the OpenSim inverse kinematic algorithm with equation 4. The complexity of the shoulder consists in the number of degrees of freedom that every joint. Therefore, the glenohumeral joint has three outputs, one for every degree of freedom.

4.2.5 **Inverse dynamics implementation.**

The inverse dynamics solves the moments for the joints using the equation56 to find τ. Which are the moments in every joint. M, C and G are known values obtained from kinematic data The generalized coordinates are expressed as "q" and the respective first derivate is $\dot{q}$ *and the second derivate is* $\ddot{q}$.

$M(q)\ddot{q} + C(q,\dot{q}) + G(q)$+E=τ .....equation 5 [121]

Where:

$$\tau = \begin{Bmatrix} M_{Humerus-scapula} \\ M_{Scapula-thorax} \\ M_{Thorax-humerus} \end{Bmatrix}$$

The moments are calculated for every joint. Every joint is restrained by a coordinate limit force (CLF), which allows to calculates the sum of torques that restraint the joint [116], with damping forces for every (DOF) and for every joint. The mechanical properties are defined in *Table 5* in the appendix.

The moments are evaluated for the GHJ with equation 6. A moment (τ) is estimated for every DOF of the shoulder joint. The CLF, muscle and tendon parameters were obtained from the literature, where they had been calculated with a benchmarking simulation[89] and Rankin's experiments[122].

4.2.6 **Joint reaction forces implementation**

Joint reaction forces are estimated in the internal joint structures and are applied because of all the loads that are acting in the model. The joint reaction forces simulate joint structures that are not included in the model, for instances: ligaments, cartilage, and soft tissue. The

joint reaction forces are expressed in the joint centre of the parent and child reference systems [123].. To represent these forces that are applied in a system, Newton defined dynamic equation 6:

$$\sum_{i=1}^{p} \vec{F_i} = m\vec{a} \qquad equation\ 6$$

The equations of the models are based on Newton's second law of inertia, which is described with a linear relationship between acceleration and force. Position can be computed in a time sequence. With this reference translations and rotations can be measured between rigid bodies. For example, the shoulder joint can be defined as a linkage.

$$\sum \vec{F}_{external} + \sum \vec{F}_{muscles}\left(\vec{F}_{GH}, \vec{F}_{SC}, \vec{F}_{jj}\right) + \sum \vec{F}_{constraint} + R_i = M_i a_i.. \quad equation\ 7$$

$$R_i\ (Joint\ reaction\ Forces)$$

$$\overrightarrow{F_{GH}}\ (Glenohumeral\ contact\ force)$$

$$\overrightarrow{F_{SC}}\ (Sternoclavicular\ force)$$

The musculoskeletal models´ joint reaction forces are the sum of the muscle forces " $\vec{F}_{muscles}$" and the other forces expressed in equation 7. The number of forces is higher than the numbers of degrees of freedom. This leads to a mechanical redundancy, that requires the use of a static optimization algorithm. The static optimization algorithm calculates a unique solution to this redundancy.

4.3 Data processing

The experimental motion capture data processing was done following the steps described in Figure 25. The experimental motion capture data was exported to OpenSim for the Holzbaur and the WU model.

4.3.1 Kinematic data

4.3.1.1 Scaling

Both models were scaled with the measurement-based scaling method with OpenSim. The thorax, humerus and scapular were scaled for length, width, and height of every segment[97]. The ulna, radius and clavicle were scaled with only the length between the proximal and distal

markers. The bony landmarks were scaled with OpenSim scaling tool with a ten static pose weight and the markers with a lower confidence were with static pose weights of 5 and 1.

4.3.1.2 Data Processing

Kinematic data of three cycles was filtered in MATLAB 2021b with a 5 grade Savitzky–Golay filter with a 0.05 smoothing factor [124]. The filtered and raw data is shown in Figure 26

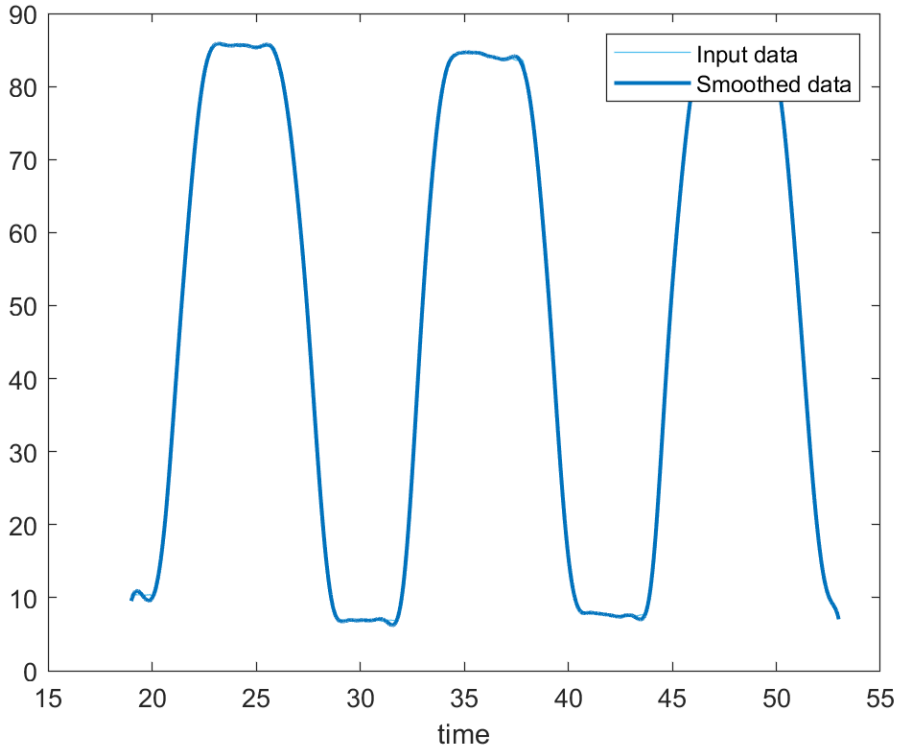

Figure 26. Filtered and raw data of thoracohumeral elevation of three cycles of 1 participant

4.3.1.3 Transformation to ISB recommendations conventions

The filtered inverse kinematic data was transformed to the ISB recommendations with the equations 3 to equation 3.C. The transformation of the Holzbaur model to the ISB recommendations was made to compare joint kinematics between both models.as shown in.

Figure 27

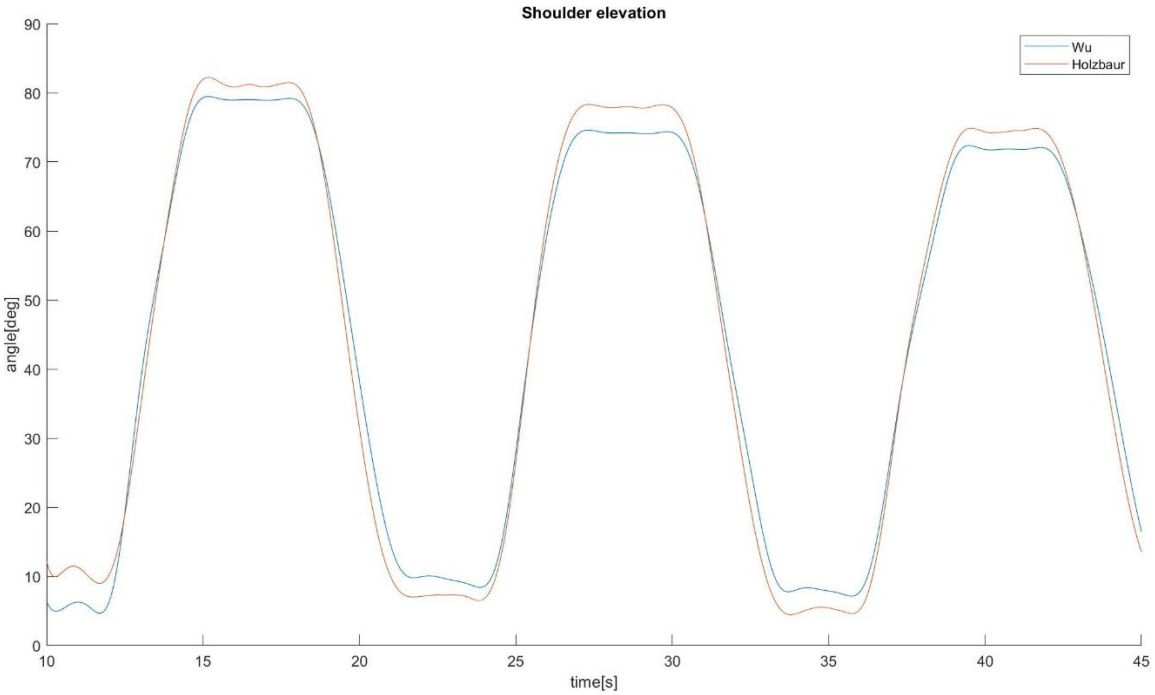

Figure 27.Shoulder elevation, for the Holzbaur and Wu model for three cycles

After calculating the mean for the three the cycles of thoracohumeral angle the graphs can be shown in Figure 28. The 3 cycles were interpolated with a cubic spline function in MATLAB 2021 b, and normalized in the horizontal axis from 0 to 100% of cycle of time, that is shown in the Figure 28Figure 28

.

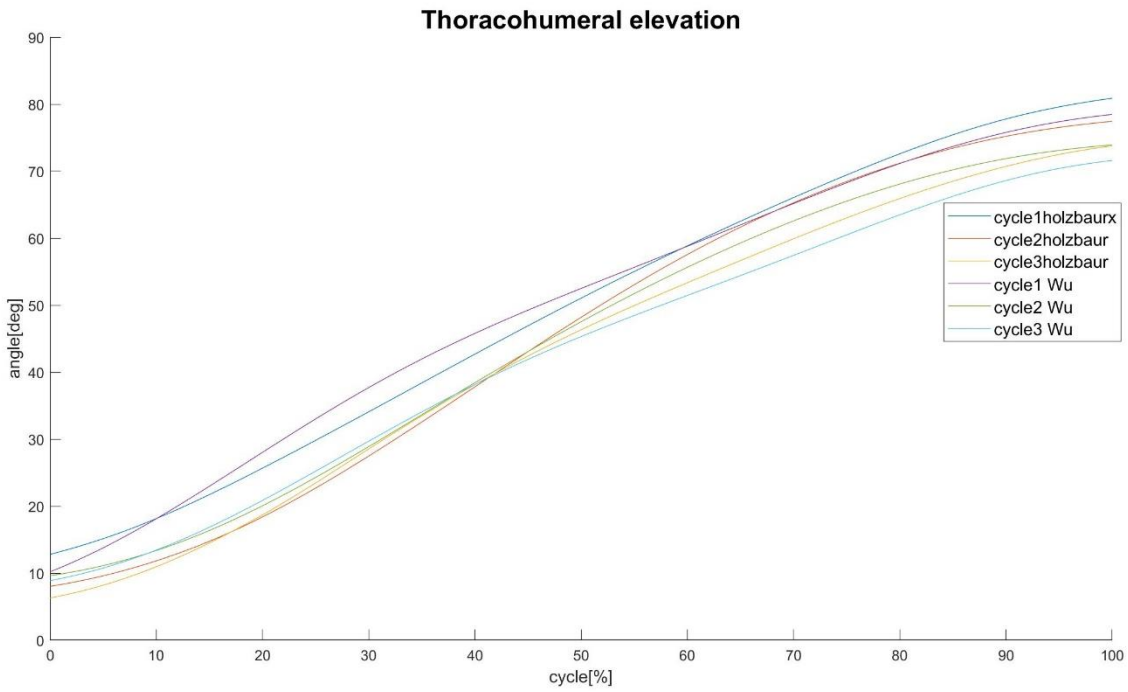

Figure 28. Thoracohumeral angle vs time for three cycles for Wu and Holzbaur model

The Figure 28 shows the thoracohumeral angle, which is the main angle of rotation for the motion that was captured for the eight participants. All the participants realized a 90-degree abduction from the resting position to the 90-degree thoracohumeral elevation. If the participants were not able to do a 90-degree thoracohumeral elevation, no feedback was provided to the participants to ensure the most similar motion to daily life activities was recorded. Therefore, the range of motion was not always ending in 90 Degrees for all the participants. The standard deviation was calculated for the three cycles for every subject as shown in Figure 29.

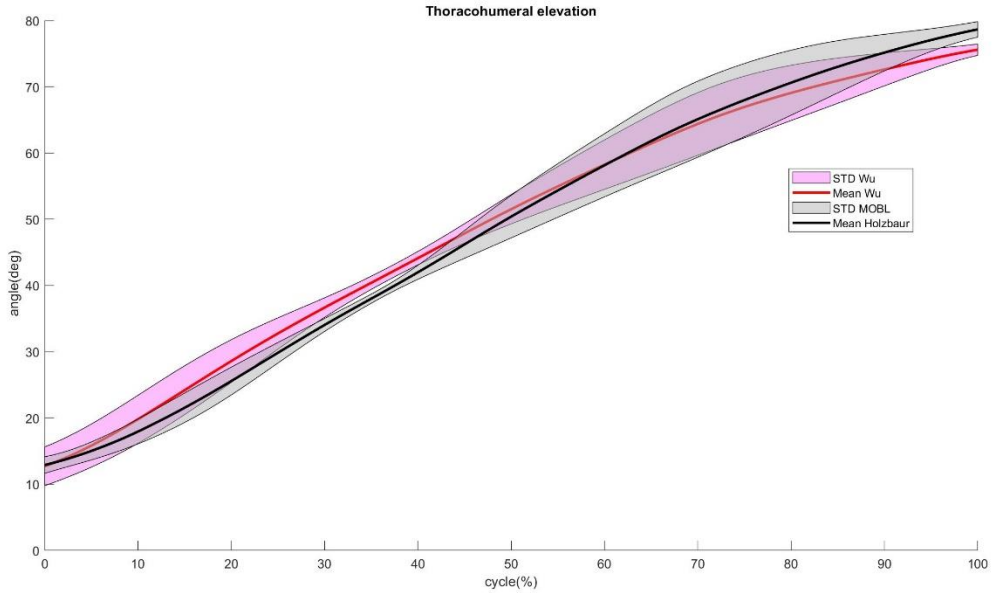

Figure 29. Mean thoracohumeral angle vs. time cycle

The Figure 29 is an example of the plot that was made for the eight subjects for every degree of freedom. The kinematics helps understand the variations between models for every subject.

4.3.2 **Dynamic Data**

The Inverse dynamics algorithm was applied in OpenSim to calculate the thoracohumeral elevation moment, thoracohumeral elevation plane moment and the shoulder rotation moment with a two [Hz] Butterworth filter that is applied in OpenSim. The resultant moment was calculated for both models as shown in

Figure 30.

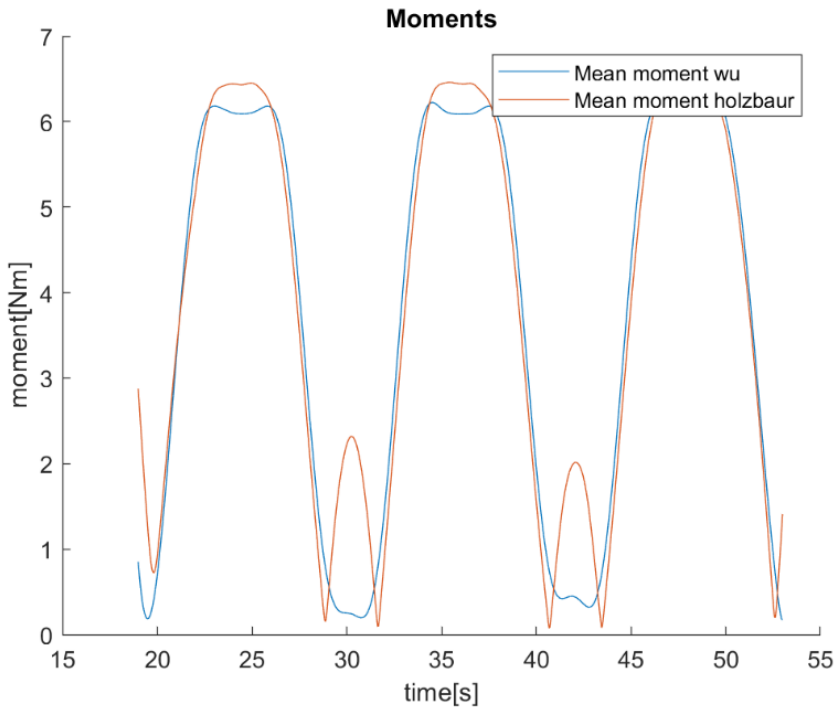

Figure 30. Resultant moment for 3 cycles for a participant

The resultant moments were segmented for the elevation phase with the same time segments that were used with the inverse kinematics data. The data was normalized in percent of time cycle time from 0 to 100% with a cubic spline function in MATLAB, the resultant moments for one participant are shown in Figure 31.

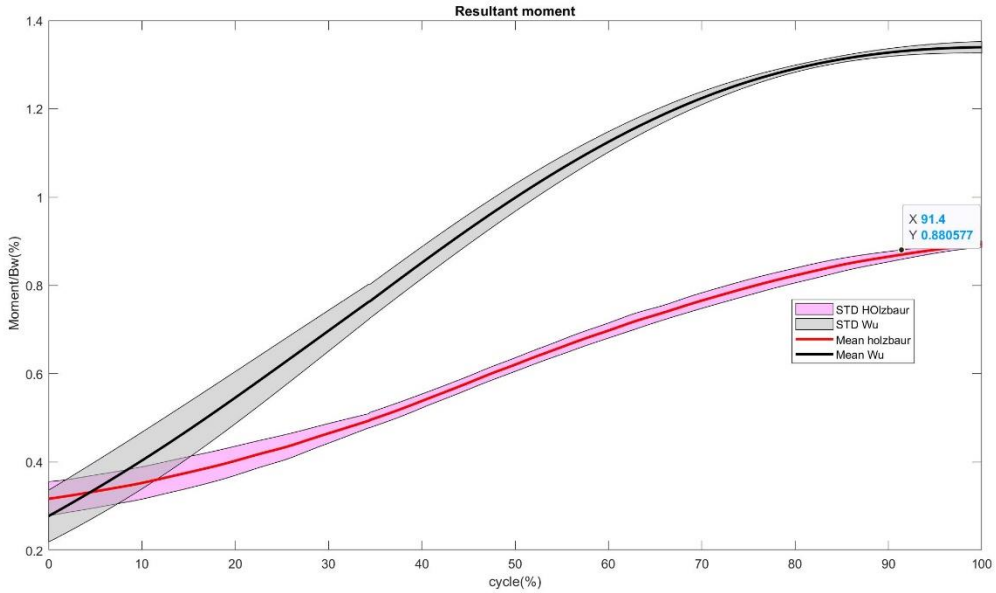

Figure 31. Mean Joint moments for resultant moment force for the Holzbaur and Wu model

The Figure 31 shows the comparison between the Wu and Holzbaur model to calculate the joint moments with the inverse dynamic algorithm with OpenSim. This figure can provide information of the angles of the thoracohumeral joint during motion. The differences can be detected for every participant for both models. The standard deviation of the resultant moment is high at the beginning because the thoracohumeral plane and shoulder rotation moment have wide variation in the first 10 degrees of motion for both models

5 RESULTS

5.1 Kinematics

The joint kinematics has been used to detect differences between healthy and pathological subjects. In this research eight healthy subjects did three cycles that attempted to do a 90-degree thoracohumeral elevation were the participants attempted to do motion in the sagittal plane. The sagittal plane is parallel to the thorax of the subject.

Figure 32 shows the mean for three cycles for eight subjects that realized a thoracohumeral elevation. To calculate the mean angles, first the mean data was calculated for the 3 cycles. After calculating the mean of the 3 cycles, the mean was calculated for the 8 subjects. Therefore, the kinematic data is the mean of the 3 cycles for the 8 participants.

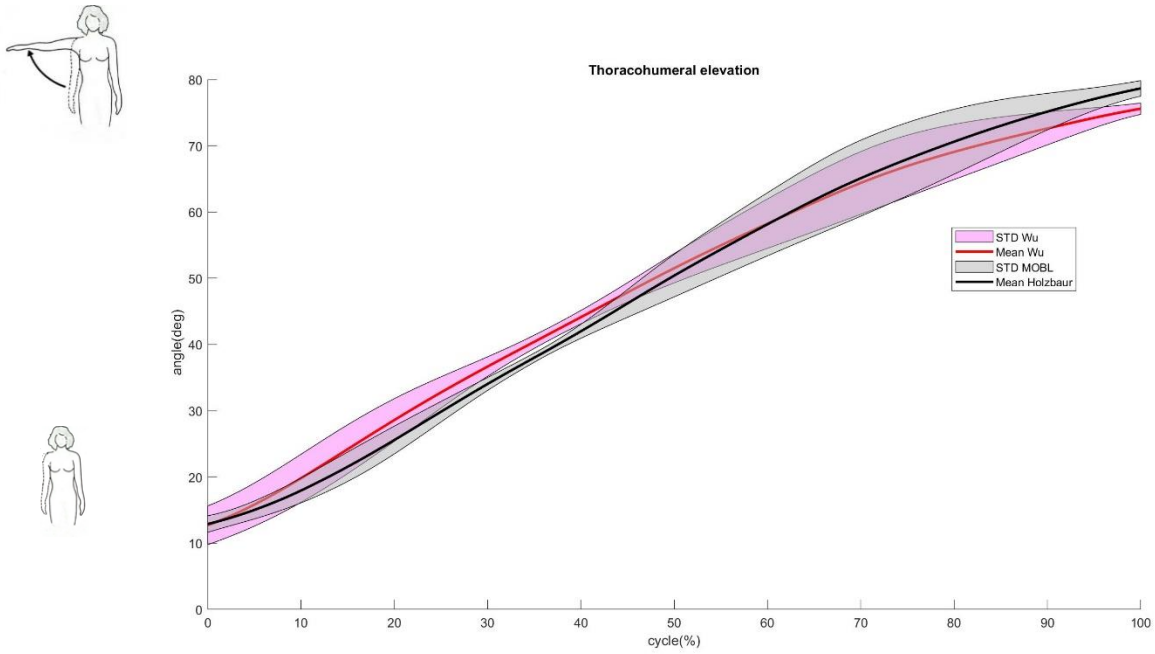

Figure 32. Mean thoracohumeral plane for three cycles of 8 participants

The positive thoracohumeral elevation is described as an elevation of the humerus relative to the thorax. The zero angle of thoracohumeral elevation is described when a subject has the humerus horizontal to the vertical axis of the thorax. Both models show an increase in angle

during cycle time. Nevertheless, the mean range of motion for the Holzbaur model was 72 degrees and of 65.32 degrees for the Wu model. This shows that different algorithms have different range of motion for a mean thoracohumeral elevation angle. For instance, the Holzbaur model has a lower initial angle and a higher ending angle, in consequence the Holzbaur model has a wider range of motion with the same experimental data. The ranges of motion and the angles in both models were consistent with the literature for this motion. Nevertheless, the standard deviation was higher for both models after the 50 degrees of thoracohumeral elevation due to the intracycle and intrasubject variation of range of motion between 50 and 90 percent of the cycle.

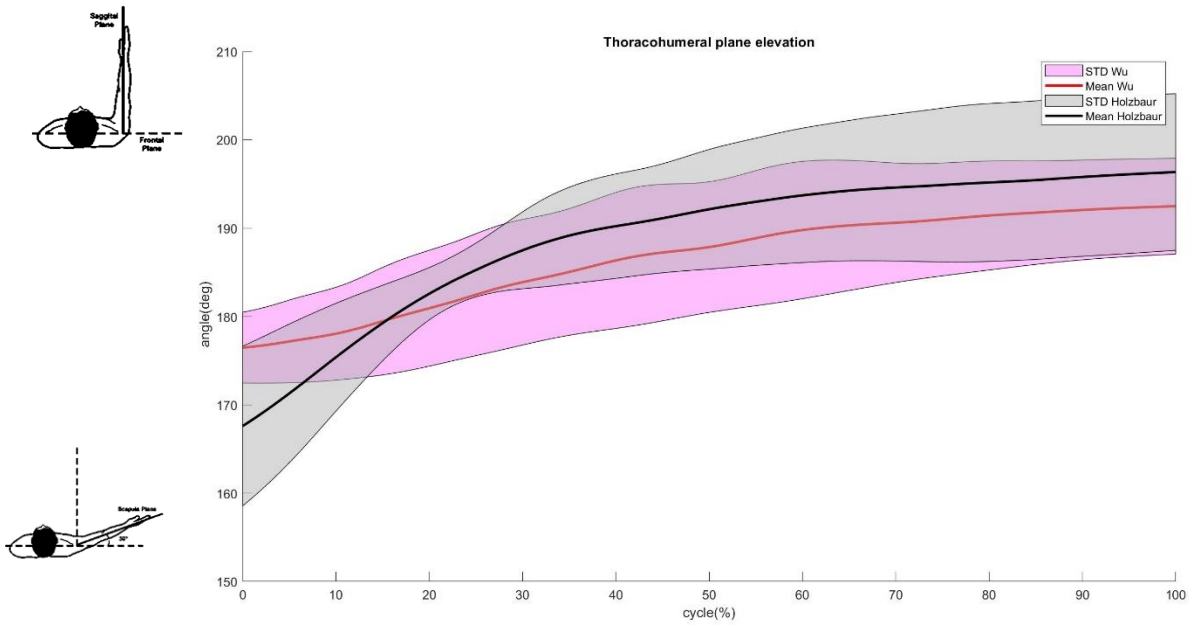

Figure 33 Mean thoracohumeral plane elevation vs. cycle for 3 cycles of 8 participants

The positive thoracohumeral plane angle represented in

Figure 33 describes a motion of the humerus going in an anticlockwise with as shown in the left side of the vertical axis of

Figure 33. The mean range of motion for the Holzbaur model was of 23.19 degrees for eight subjects. The mean range of motion for the Holzbaur model was of 17.9 Degrees for the same eight subjects. The variations in the standard deviation are higher than in the shoulder plane of elevation. This is caused by a larger variation for each subject for both models. The increase

in the standard deviation compared to the thoracohumeral angle is higher due variation of a thoracohumeral plane elevation during the thoracohumeral elevation.

The participants did not receive corrective feedback if they deviated from the requested motion. Some participants did a slight positive rotation in the thoracohumeral plane angle when the shoulder was elevated Therefore, the participants had a high standard deviation in all the ranges of motion. The variation of the mean thoracohumeral plane elevation between cycles and subjects is also affected by the skin motion artifact in the scapula. The

Figure 33 shows for all the participants the shoulder elevation increased together with thoracohumeral plane elevation. In future research it will be necessary to make corrections to every subject to have a more accurate comparison between participants.

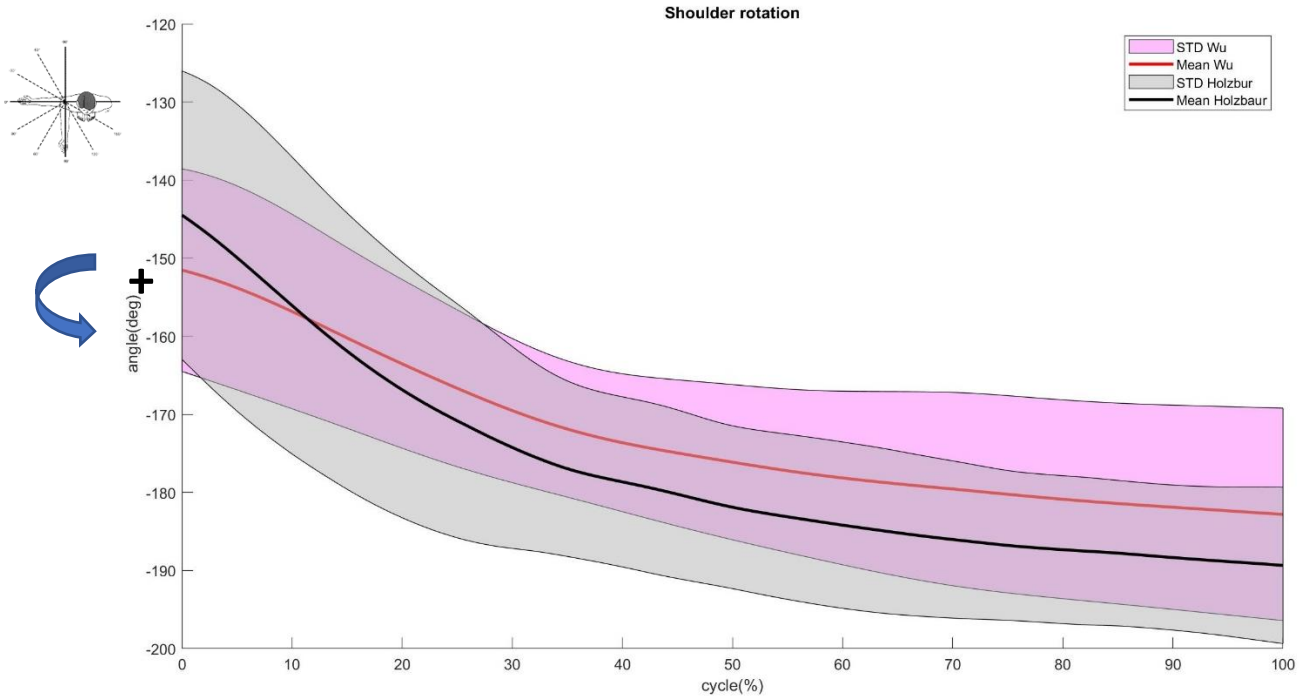

Figure 34. Shoulder rotation angle for 3 cycles for eight subjects

The glenohumeral rotation is the motion of the humerus relative to the scapula. The glenohumeral rotation is colinear with the axial axis of the humerus. The positive direction

occurs with an anticlockwise rotation that is represented with a blue arrow at the left side of the vertical axis of the

Figure 34. For both models (Wu and Holzbaur) a thoracohumeral elevation is accompanied with an external rotation, which would be represented with a clockwise rotation seen from a superior view. The range of motion of the mean external rotations is of 49.62 degrees for the Holzbaur model, and of 24.9 degrees for the Wu model. The difference in range of motion was detected with all the subjects, this means that the Holzbaur model has higher external rotation during motion. The difference is caused by two different approaches to simulate the motion of the scapula. The Holzbaur model uses a linear regression [108], meanwhile the Wu model uses a shoulder plane constraint [115]. These variations have different results which would need the use of other methods to validate that the models are able to detect accurately the position of the scapula during motion. In this research we did not have any evidence to prove that the shoulder rotation was accurate enough to detect the position of the scapula and the humerus during motion. The behavior of the shoulder rotation was consistent with the literature, because the shoulder rotates externally when it has a positive thoracohumeral elevation [125]. Further research is needed to calculate the relative error of the glenohumeral rotation to understand the great variations in the glenohumeral rotation for all the cycles and participants.

5.2 **Dynamics**

After estimating the joint kinematics, the dynamics were calculated. The joint moments and internal forces were estimated with anthropometric values, inertial properties and mechanical properties that are reported in the literature for the Wu[115] and Holzbaur model[89]. The mass and inertial moments of the bones were similar for both models. The main goal of the next section was not to increase the accuracy of the model but to replicate the methods that were reported in the literature for every model and calculate the differences with biomodular implants reported in the literature[82,126]. The mass of the humerus, thorax, clavicle and scapula were calculated from the literature based on the mass of the complete body for every participant[127].

The moments were normalized dividing by the mass in Newtons [N] for every subject with the same method than the authors that used biomodular implants[36]. The body mass was

multiplicated by 9.81 $\left[\frac{m}{s^2}\right]$. The force is expressed in percent [%]. The moment was also divided by the mass of the subject expressed in newtons which results in a percent multiplied by mass as shown in the equation 8.

$\frac{Moment[Nm](100)}{Bodyweight[N]}$=Normalized Moment (BW[%m]) ……Equation 8

5.3 **Joint moments**

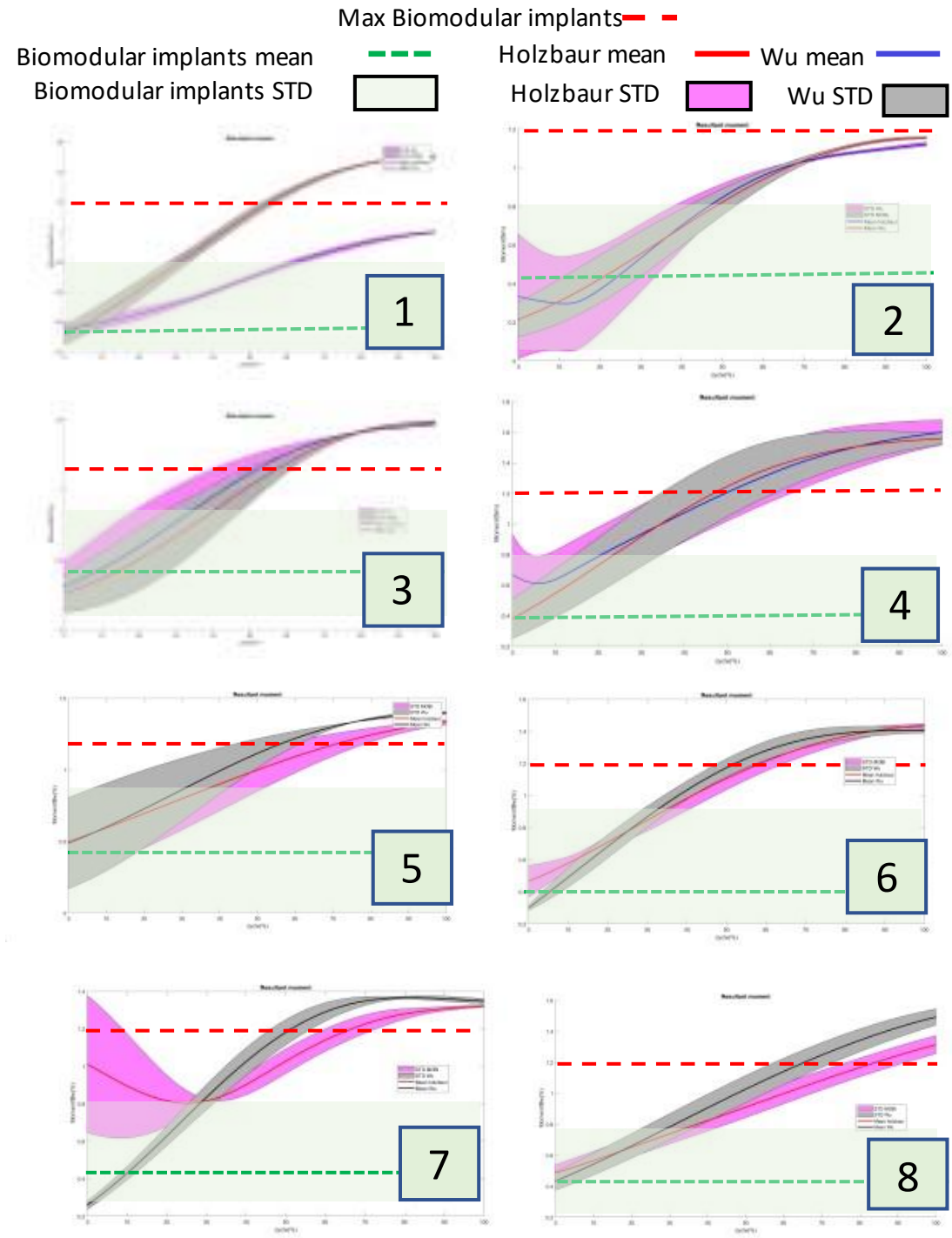

Figure 35 Joint moments for Holzbaur and WU model for eight participants

After computing the joint kinematics, the inverse dynamic algorithm was applied in OpenSim as shown in the methods section. The data was sampled in time cycles with MATLAB cubic splines. The time segments were sampled with the same initial and final time than for the kinematics results in the last section.

The green dashed line in Figure 36 represents the mean peak resultant moments that were directly measured with biomodular implants [36,82]. For the eight subjects the Holzbaur and Wu model overestimated the value compared with the mean value of bio-modular implants. The differences for the biomodular implants of peak resultant moments are from 0.1 to 1.2 %Bwm [1] which are shown in the red dashed line in Figure 36. The great differences between subjects also show that the joint moments have a great variability with direct measurement that can be ten times higher from one subject to another. One of the limitations of the experimental results done with biomodular implants, is that the author only divides his tests in slow and fast movement. A lack of quantitative parameters to measure the speed of the motion makes difficult to compare the data with the findings on this research.

Therefore, the Wu and Holzbaur models were compared with both: the fast and slow motions reported in the literature [36]. The results show that for the eight subjects, all the graphs show a similar incremental curve with time, except for the 7^{th} participant. The 7^{th} participant showed a higher increase in the external rotation during motion. The changes in shoulder rotation and thoracohumeral elevation caused the main difference between the Holzbaur model and the Wu model. There was no evidence that one model has higher values for resultant moment for all the subjects. The greatest variations between the Wu and Holzbaur model for the peak resultant moments were found for the first participant as shown in Figure 36. The green dashed line represents the average peak moment in 90 degrees of thoracohumeral elevation. Therefore, the moments estimated with the Wu and Holzbaur models are significantly higher than the values the mean resultant moments that are reported with the direct measurement made with biomodular implants [36]. Nevertheless, this research requires more information from the kinematics of the subjects that were evaluated with biomodular implants to understand the cause of the great differences between different subjects.

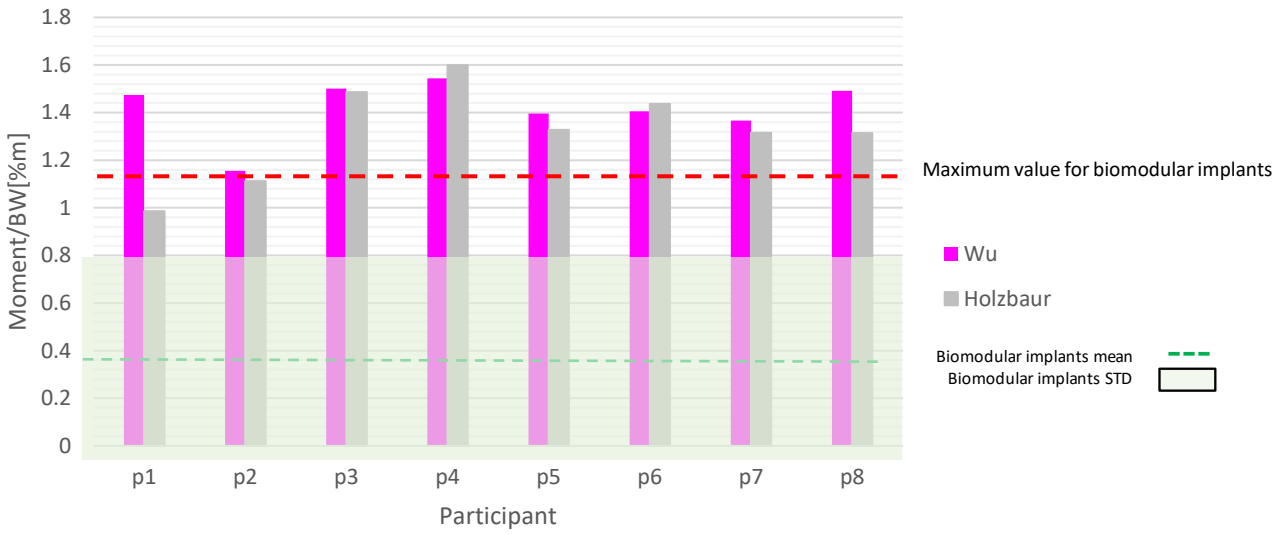

Figure 36. Glenohumeral joint Moment/BW% vs time for eight participants

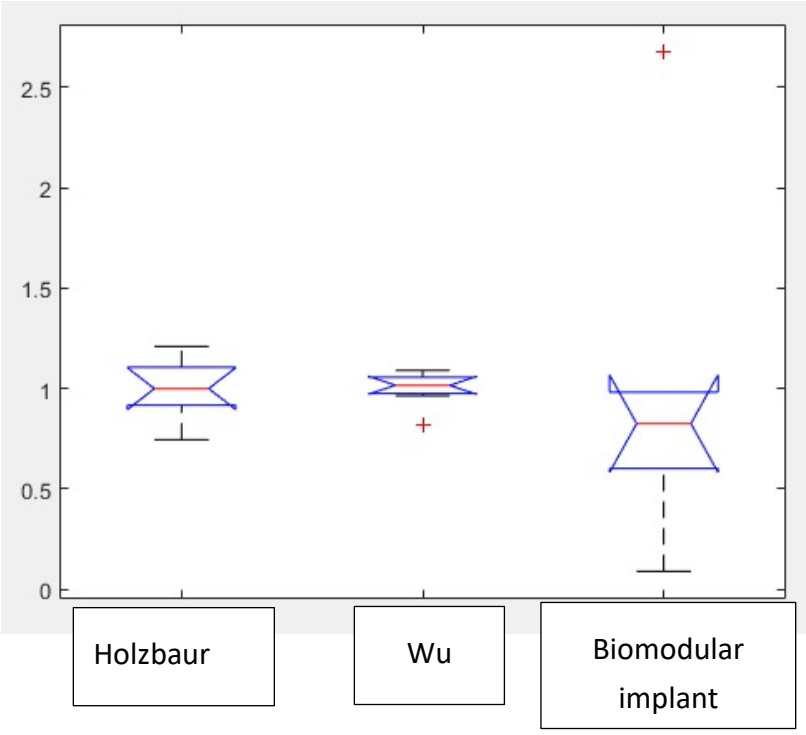

Figure 37. Box plot for the joint moments for Wu and, Holzbaur and biomodular implants

A Kruskal-Wallis test was applied in MATLAB for the Wu, the Holzbaur and the biomodular implants. These results show the 25% 50% and 75% of percentile for each population. From

the models, the Holzbaur models has the wider variation, meanwhile the Wu has the smaller variation between the 25% and 75% percentile. The

Figure 37 shows also that the highest dispersion exists in biomodular implants that were evaluated with 6 participants in the literature [1]. Nevertheless, there is not enough information in the research to know the cause of the variations in the measurements done with biomodular implants. The author's hypothesis is that the friction has wide variation between subjects and this causes high differences in joint contact forces and joint moments [36]. The measurements done with biomodular implants have the highest dispersion coefficients that are observed in Figure 38. The wide dispersion coefficients in the measurement of the joint moments in the biomodular implants can be caused of the lack of measurement of the angular speed for every cycle and participant.

The Kolmogorov-Smirnoff tests were applied for the Holzbaur model, Wu model and biomodular implants.

Kolmogorov-Smirniov Normality Test for one universe

		MoblNormalized	wuNormlaized	Biomodularlmplant
Frecuencies		8	8	6
Normal parametres[a,b]	Mean	1.3218	1.4169	.4483
	Std. Deviation	.19790	.12208	.39640
Maximum extremal differences	Absolute	.233	.214	.342
	Positive	.115	.148	.342
	Negative	-.233	-.214	-.160
Statistical test parametre		.233	.214	.342
p Value (two-tailed asymptotic)		.200[c,d]	.200[c,d]	.027[c]

a. Test distribution is Normal
b. Calculated based on data provided
c. Significance correction of Lilliefors
d. That is an inferior limit of the true significance

Figure 38. Kolmogorov-Smirnov normality test

The Holzbaur and Wu joint moments had values that are close to have a normal distribution. In contrast, the biomodular implants shows a behaviour that is not close to a normal distribution of data. This means that the biomodular implants have the highest differences in

the joint moments between the mean values for all the participants. The ideal way to improve this research is to increase the sample of participants with biomodular implants. However, it is difficult to have a high sample of subjects that can have a surgical procedure with a biomodular implant. Based on previous research the best way to improve the existing data is to increase to more than 30 samples of each test to reduce data dispersion and analyse data according to normal data distribution [128].

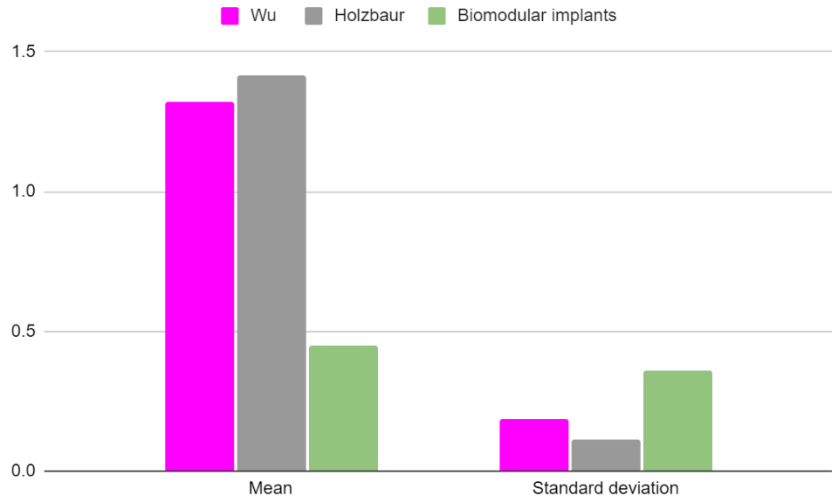

Figure 39. Standard deviation of resultant mean peak joint moments for Wu Holzbaur models and biomodular implants

For the estimation of joint moments with the musculoskeletal models the inertial properties of the shoulder require verification and validation because any difference in the inertial properties has a high influence over the inverse dynamics data. Same happens with the morphological characteristics that could be caused using scaling the segments of the generic models.

Figure 39 show the differences of the dispersion coefficient and standard deviation between both models and the biomodular implants. These results are consistent with the values obtained with the Kruskal-Wallis test.

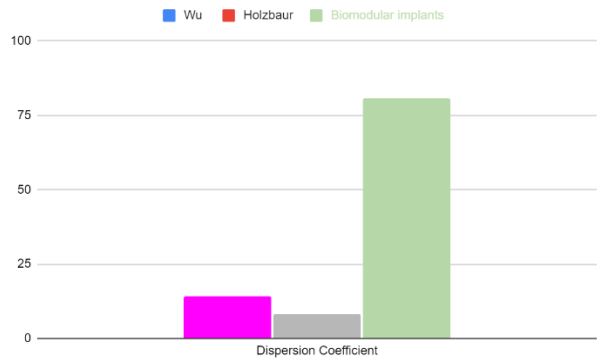

Figure 40.Dispersion coefficient

The Wu model exhibit less dispersion of the three models analysed because the data contained in the Wu model are closer to the mean values. However, as the Holzbaur model, it shows a tendency to obtain values under the mean. After applying the Fisher value, the findings are that he differences between variance of both distributions is not significative.

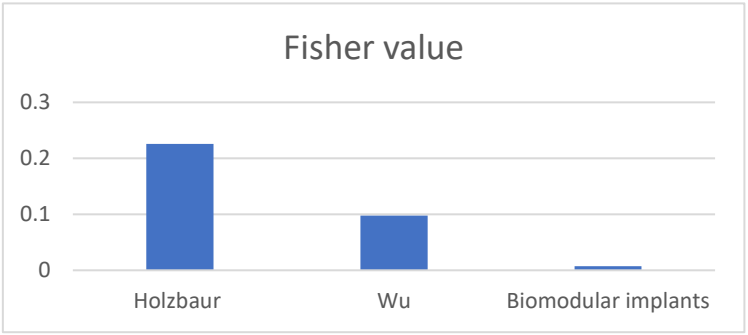

Figure 41. Fisher test for peak joint moments for Holzbaur Wu and biomodular implants

Even if the biomodular implants are reported to be the gold standard to measure joint moments, the fisher test shown in

Figure 41 together with the results of the t value in the

Table 3 show that there are not statistically significant differences between the Wu model, the Holzbaur model and the biomodular implants to measure resultant peak moments due to the small difference between the fisher value between Holzbaur and Wu model.

Model	Holzbaur vs Wu	Holzbaur vs biomodular implants	Wu vs, Biomodular implants
t test value	0.2706	0.0017	0.0013

Table 3. T test for Holzbaur and Wu and biomodular implants

5.4 Joint reaction forces

The joint reaction forces were calculated with the muscle parameters from Wu [115] and Holzbaur [116] that are used by default in OpenSim. The joint reaction forces were calculated with the static optimization results without using the force- length velocity curves. The results of our research for the muscle forces did not have consistency with the literature. The models that were used with the mechanical properties reported in the literature presented a wide variation between subjects from 4 to 100 N for the muscle forces. This leaded to high variations in the glenohumeral joint contact forces.

In contrast with the resultant joint moments, the mean peak joint resultant forces were sub estimated with the Wu and Holzbaur models compared with biomodular implants. The mean of peak joint reaction forces in a 90-degree thoracohumeral elevation are 66.5% for biomodular implants. For the Holzbaur model the mean peak resultant joint contact forces were 45% for the three cycles for 8 subjects. The Wu model had a mean peak joint contact forces of 25.95% for three cycles of 8 subjects.

The

Figure 42 shows the great differences between the Wu and the Holzbaur model One of the most crucial factors that must be considered is that the Holzbaur models includes more thoracohumeral muscles than the Wu model

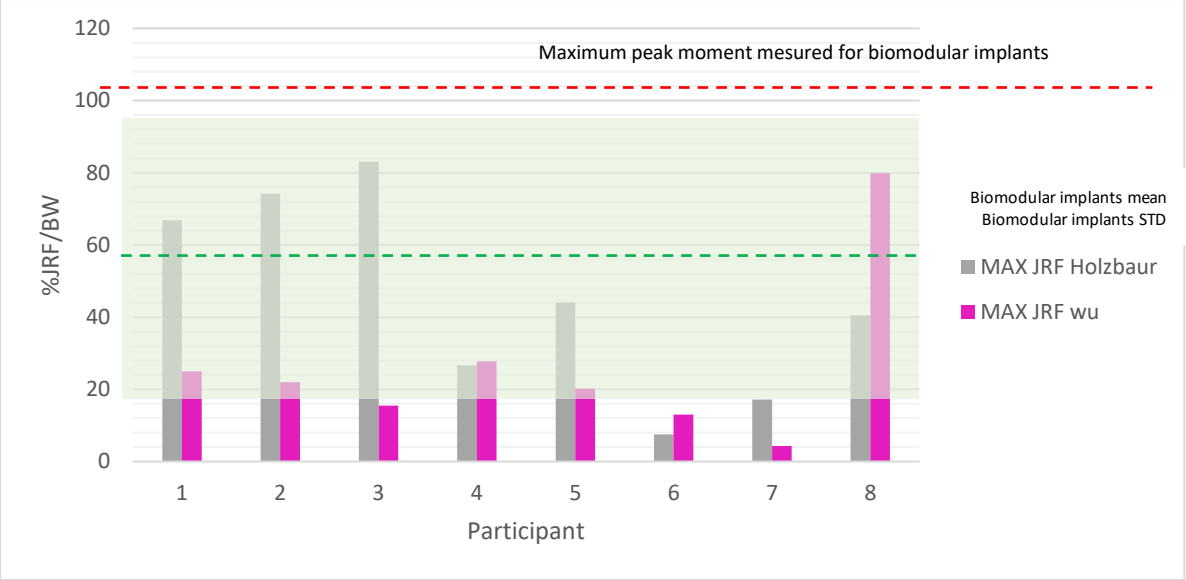

Figure 42. Resultant joint reaction forces for thoracohumeral elevation of 8 participants for three cycles of thoracohumeral elevation

The research done with biomodular implants showed variations from 50 to 100 % of peak resultant joint contact forces for a slow thoracohumeral elevation and from 40 to 100 % of force for a fast thoracohumeral elevation. The measurements done with biomodular implants have a lack of quantitative measurement of the joint kinematics. Therefore, our research cannot compare the joint reaction forces that were estimated with musculoskeletal models with the joint reaction forces measured directly with biomodular implants because the linear and angular velocity of the glenohumeral joint were not measured during the use of biomodular implants[1]. The lack of measurement of the glenohumeral joint angles can also generate a wider variation of the joint reaction forces from one subject to another with biomodular implants. This research has shown that the musculoskeletal models need more validation and verification to accurately replicate the mechanical properties, morphology, and motion. The results of this research show that to have a better simulation, it is necessary to adapt better the muscle mechanical properties from the default values that are in the literature and that are used as default values in OPENSIM.

6 DISCUSSION

The musculoskeletal models are the only non- intrusive method that can estimate muscle forces, joint contact forces and joint moments simultaneously. Nevertheless, the estimation of the joint contact forces relies in the accuracy of the marker placement to detect the position of the anatomical skin mounted landmarks. The joint coordinate systems are calculated based on the position of the anatomical landmarks. The soft tissue artifact is the error caused due to the relative motion of the skin mounted markers relative to the anatomical landmarks. The first limitation of this research is that there was no method to evaluate the accuracy of the skin markers to detect anatomical landmarks during motion. This means that the position of the scapula and humerus can have errors that affect all the process to calculate the joint contact forces and moments that have been reported by other authors to have 23% of relative error [110]. The use of magnetic resonance imaging MRI is a tool that has been recommended by researchers to measure the relative error of the marker placement to improve the accuracy of the kinematic and dynamics. The researchers have used the virtual markers placement based on the MRI to improve the accuracy to calculate the joint coordinate systems of the glenohumeral joint [73,129].

The second limitation was the lack of knowledge of the accuracy of the estimation of the inertial properties from the segments that were used for the inverse dynamics, static optimization, and estimation of the joint contact forces. The inertial properties of both models are based on a generic model for a European male and were scaled based on linear regressions. There is no evidence in this research to know accurately the relative error in the calculation of the joint contact forces due to the variations in morphology and mechanical properties in both models (Wu and Holzbaur). Nevertheless, the differences in the range of motion and the peak joint contact forces show the difference between both models to represent the same motion. The shoulder rotation showed a similar behavior that had been reported by other authors. Nevertheless, to know the accuracy of the range of motion during motion gold standard methods are fundamental to validate the results that were obtained with musculoskeletal models. The use of MRI and medical images can also help to use the positions of the muscle attachments and the morphology of the bones to adapt the musculoskeletal models to the subjects anthropometry and therefore the inertial properties

of the musculoskeletal model can be calculated with the 3D geometrical surfaces of the muscles and bones[130].

The third limitation is the lack of subject specific parameters to scale the muscle forces and the maximum isometric force with direct measurement of external forces. The inverse dynamics results show a similar result between subjects for every model, but the joint contact forces show a wide variation between subjects. The Wu and Holzbaur model require to be validated for a 90-degree shoulder abduction with more accurate methods. Researchers have used subject specific parameters to scale the muscle forces for every subject. The calculation of the maximum voluntary isometric contraction has been used to scale to force that acts in every muscle [115].

. A higher number of muscles influences the joint reaction forces. The thoracohumeral muscles are fundamental to stabilize the humerus relative to the thoracic cage that are listed in the

Table 4. In contrast with the Wu model, the Holzbaur model has thoracohumeral muscles and by consequence also has a higher number of muscles, therefore the joint reaction forces are higher. Another important variable is the maximum isometric force. The maximum isometric force is different for both models, and well as the number of muscles is different. The number of muscles that work in a motion change significantly the output of the joint reaction forces. The participant 1,2,3 have higher joint reaction forces in the Holzbaur model that are caused by a higher muscle force that is applied in the glenohumeral joint. For example, in the Table 4 the infraspinatus has a higher maximum isometric force for the Holzbaur model than the WU Model, therefore, the infraspinatus peak forces were higher for the Holzbaur model.

Holzbaur		Wu	
Muscle name	Maximum isometric force [N]	Muscle name	Maximum isometric force [N]
deltoid anterior	1218	deltoid anterior	556.8
deltoid medial	1103.5	deltoid medial	1098.4
deltoid posterior	1103.5	deltoid posterior	944.7
supraspinatus	499.2	supraspinatus	410.7
infraspinatus	1075.8	infraspinatus	864.6
subscapular	1306.9	subscapular	944.3
teres minus	269.5	teres minus	605.4
teres major	144	teres major	234.9
pectoral Majors 1	444.3	pectoral major	983.4
pectoral majors two	658.3	pectoral major two	699.7
pectoral Majors 3	498.1	pectoral major two	446.7
Latissimus dorsi one	290.5	Latissimus dorsi	1129.7
Latissimus dorsi two	317.5		
Latissimus dorsi three	189		
coracobrachialis	208.2	coracobrachialis	306.9
triceps longus	771.8		
triceps lateral	717.5		
triceps med	717.5		
anconeus	283.5		
Elbow supinator	379.6		
biceps long	525.1		
biceps short	316.8		
brachialis	201.6		
		rhomboid minor superior	185.9
		rhomboid minor inferior	111.57
		Elevator of scapula	301.67
		trap4	557.243
		trap3	155.28
		trap2	162.44
		trap1	280.56
		serratus one	365.11
		serratus two	179.96
		serratus three	377.92
		subclavius	195.8

Table 4. Maximum isometric force of muscles for the Holzbaur[131] **and Wu**[115] **model**

The Holzbaur model uses a linear regression to estimate the position of the scapula, humerus, clavicle, and thorax based on the position of the markers of humerus and thorax[108].

From all the standardized motions, the 90-degree thoracohumeral elevation was evaluated because this research was focused mainly to evaluate anterior-posterior GHJ instability which is detected during thoracohumeral elevation.

WU model uses a gliding plane which requires three markers in the scapula to define the plane of motion of the scapula. The same marker placement protocol was used during the motion capture for all the participants with the use of both models. Therefore, the variations in the inverse kinematics are caused by differences in the placement of the virtual markers in the musculoskeletal model and the differences in the algorithms to detect the scapula and humerus for the Wu and the Holzbaur model. The Wu model has wider standard deviation for the shoulder rotation and the thoracohumeral elevation plane because the algorithm of Wu predicts the position of the scapula based on the assumption that the scapula moves in a plane, which is not always accurate during motion. Nevertheless, the Wu model showed a higher repeatability between cycles and subjects than the Holzbaur Model.

Both models have a different range of motion of the scapula, humerus, clavicle, and thorax. Therefore, the length of the muscles changes during motion due to the relative motion between the bones. The muscles have a force-length-velocity curve that have variations with the length. The muscle forces are highly influenced by the origin and insertion of muscles in the musculoskeletal models and in the participants morphology. Both models have different position for the muscle origin and insertions and are affected by the inertial properties. Therefore, the use of MRI can help to improve the accuracy to replicate the shoulder musculoskeletal morphology.

This research found that the existing results done with biomodular implants shows a high dispersion in the joint moments, the authors explain that the wide variation is caused by the differences in friction in the prosthesis between subjects. Therefore, this research was not able to evaluate accurately which MSK model had a higher accuracy compared with biomodular implants. Nevertheless. the contribution in this research was detecting that the generic static optimization methods that are used by default in OpenSim did not have consistent results with the literature for the joint moments and joint reaction forces[109]. The joint moments were higher for the MSK models and the joint reaction forces did not have similar results to the biomodular implants, which is the most accurate method to measure

joint reaction forces directly in-vivo. It is important to highlight that the research done with biomodular implants was evaluated with elderly participants, in contrast the research we made with musculoskeletal models was done with participants with a mean age of 41. It is complex to calculate accurately the muscle forces with non-intrusive methods but a progress in the existing work would be to have consistent muscle forces that were reported in the literature[115].

7 CONCLUSION AND FUTURE WORK

The musculoskeletal models attempt to simulate the joint kinematics and dynamics based on motion capture data of reflective skin markers. The differences between both models are caused by differences in the number of muscles, the maximum isometric forces, the inertial properties, the morphology, and the algorithms to estimate the position of the scapula, humerus, and clavicle (scapular rhythm). The accuracy of the musculoskeletal models is sensible to the marker placement, the data processing, scaling, inverse kinematics, inverse dynamics, static optimization, and the calculation of the joint reaction forces. The standard deviation between the mean of the 3 cycles for the 8 participants shows the wide variation for the thoracohumeral elevation plane and shoulder rotation. The Holzbaur model shows a higher inter-cycle and inter-subject variation of the standard deviation for shoulder elevation plane and shoulder rotation. The Holzbaur model has higher ranges of motion for the thoracohumeral plane and shoulder rotation caused by the scapular rhythm algorithms. The main differences in the joint kinematics were shown for the thoracohumeral plane elevation and the shoulder rotation for all the subjects and cycles. For both models, the highest variation for the mean range of motion for the three cycles and the eight subjects was demonstrated to be for the shoulder rotation. The shoulder rotation depends completely on the estimation of the scapula for both models. The greatest challenge for all the existing musculoskeletal models is the estimation of the position of the scapula and humerus. The future work for this research is to measure the accuracy of musculoskeletal models to estimate the position of the scapula compared with gold standard methods. Another area of opportunity is for the detection of the humerus head centre[130]. The detection of the humerus head can be contrasted with medical imaging to improve the accuracy of current musculoskeletal modelling[52].

Previous research has been done with intracortical pins [132], nevertheless the intra cortical pins have been demonstrated to change motion patterns caused by the participants pain [133]. The use of medical imaging has shown promising results without having the risks of surgical procedures [17,26,66,73]. The main goal for future research for the joint kinematics is to validate the position of humerus head and glenoid with non-intrusive methods. For the joint kinematics it is difficult to know which model replicates more accurately the motion of the scapula, therefore this research helps to understand the main differences between both

models. Future research is needed to measure the relative error of both models with a gold standard method. This research found that the generic models are not able to simulate the joint reaction forces with muscle mechanical properties that are reported in the literature, which are the default values for the OpenSIm generic models[116]. The contribution of this research is to detect that the generic models require subject specific parameters that have a better estimation of the muscle forces based on the direct measurement of the net maximum isometric force for the range of motion that are recommended to be evaluated with the motion capture system data. For example, in shoulder abduction, the maximum net isometric force can be evaluated to scale the maximum isometric force with the muscles that are activated during motion. Authors have recommended to use Electromyography to measure the muscle activation [30,96]. Another static optimization strategy will be essential to improve the estimation of the joint contact forces and muscles forces for both models.

The inverse dynamics test helped to find the joint moments for every degree of freedom for the thoracohumeral joint and shoulder. The resultant peak joint moments showed similarity in the range of values between both models compared with the great differences between the joint contact forces for the 3 cycles of the 8 participants. The mean peak joint moments for the eight participants had the lowest standard deviation, therefore the calculation of joint moments for a larger population can be evaluated to improve the statistical analysis. Based on our statistic results the Wu and Holzbaur model could be studied for more than thirty subjects to have a better statistical sample to detect differences between both models. This research detected the need of searching gold standard methods that can evaluate a higher group of patients than the biomodular implants or the use of intracortical pins. The use of biomodular implants is not accessible to a wide population. Further research is needed to know if the joint reaction forces that have been measured with patients with total shoulder replacement have similarity with a healthy population to avoid surgical intervention for diagnosis.

The main limitation of this research is the lack of methods to validate the muscle forces and mechanical properties of both models. Nevertheless, the comparison with biomodular implants demonstrates that the joint contact forces and static optimization techniques require further validation and research about the cause to study the relationship between the effect of the mechanical properties of each muscle for both models.

The future work is to determine the accuracy of inverse kinematics for the scaling and the marker placement with medical imaging. The inverse dynamics requires a validation of the inertial properties of the segments. The joint reaction forces would need to evaluate the use of medical images and of EMG and other techniques to verify the accuracy of the muscle activation and to improve the estimation of the muscle forces. Another objective to improve the comparison of both models is the application of a sensitivity and repeatability analysis between cycles and participants.

This research also highlighted the need to find a higher sample of gold standard GHJ contact forces in the literature during a shoulder abduction to meet the criteria that is recommended for statistical parameters [134]. Therefore, there is not enough evidence with the estimation of joint moments and joint reaction forces to determine the best model to evaluate glenohumeral instability based on the comparison between musculoskeletal models and the results found in the literature with biomodular implants[36]. More research is needed to improve the validation and verification of the musculoskeletal models to be able to differentiate joint kinematics and dynamics between healthy and pathological subjects. The best way to improve the accuracy of musculoskeletal models requires research of methods that replicate the joint kinematics, the estimation of muscle forces and the methods to calibrate the measurements for a higher sample of participants. This study showed joint kinematics results and inverse dynamics results that are consistent with the motion patterns that are described in the literature. Nevertheless, the peak values for the joint moments and joint reaction forces do not show similar results during thoracohumeral elevation. But this research requires collaboration with clinicians to be applied in a clinical context. This research had the limitation of not having feedback from clinicians. Therefore, a future work in biomechanics of the glenohumeral joint would need a multidisciplinary collaboration to be able to understand better the needs of patients. The shoulder joint does not have the amount of research that is necessary to be able to provide of non-intrusive methods that can replace the intrusive methods, this is a challenge that will need a detailed study of the application of biomechanics in the clinical practices for different regions of the world.

8 REFERENCES

1. BERGMANN, G., GRAICHEN, F., BENDER, A., ROHLMANN, A., HALDER, A., BEIER, A. and WESTERHOFF, P. In vivo gleno-humeral joint loads during forward flexion and abduction. *Journal of Biomechanics* [online]. 2011. Vol. 44, no. 8, p. 1543–1552.

2. NIKOOYAN, A. A., VEEGER, H. E.J., WESTERHOFF, P., GRAICHEN, F., BERGMANN, G. and VAN DER HELM, F. C.T. Validation of the Delft Shoulder and Elbow Model using in-vivo glenohumeral joint contact forces. *Journal of Biomechanics* [online]. 2010. Vol. 43, no. 15, p. 3007–3014.

3. LEDET, Eric H., D'LIMA, Darryl, WESTERHOFF, Peter, SZIVEK, John A., WACHS, Rebecca A. and BERGMANN, Georg. Implantable sensor technology: From research to clinical practice. *Journal of the American Academy of Orthopaedic Surgeons*. 2012. Vol. 20, no. 6, p. 383–392.

4. BERGMANN, G., GRAICHEN, F., BENDER, A., ROHLMANN, A., HALDER, A., BEIER, A. and WESTERHOFF, P. In vivo gleno-humeral joint loads during forward flexion and abduction. *Journal of Biomechanics* [online]. 2011. Vol. 44, no. 8, p. 1543–1552.

5. VAN DER HELM, F. C T. A finite element musculoskeletal model of the shoulder mechanism. *Journal of Biomechanics*. 1994. Vol. 27, no. 5.

6. VAN DER HELM, F. C.T. A finite element musculoskeletal model of the shoulder mechanism. *Journal of Biomechanics*. 1994. Vol. 27, no. 5.

7. KUMAR, V P. Biomechanics of the shoulder. *Annals of the Academy of Medicine, Singapore* [online]. 2002. Vol. 31, no. 5, p. 590–2.

8. TERRIER, Alexandre, AEBERHARD, Martin, MICHELLOD, Yvan, MULLHAUPT, Philippe, GILLET, Denis, FARRON, Alain and PIOLETTI, Dominique P. A musculoskeletal shoulder model based on pseudo-inverse and null-space optimization. *Medical Engineering and Physics*. 2010. Vol. 32, no. 9, p. 1050–1056.

9. OMBREGT, Ludwig. Applied anatomy of the shoulder. *A System of Orthopaedic Medicine*. 2013. P. e39–e51.

10. VEILLETTE, Christian. Scapular fractures (including glenoid). *Musculoskeletal medicine for medical doctors* [online]. 2012. [Accessed 14 November 2018].

11. PHYSIOPEDIA. Glenoid Labrum. .

12. TERRY, Glenn C and CHOPP, Thomas M. Functional {Anatomy} of the {Shoulder}A. *Journal of Athletic Training* [online]. 2000. Vol. 35, no. 3, p. 248–255.

13. RTICLE, C Redit A, WARBY, Sarah Ann, HONS, Bphysio, WATSON, Lyn, PHYSIO, Bappsci, PHYSIO, Manipulative, FORD, Jon J, PHYSIO, Bappsci, HAHNE, Andrew J, HONS, Bphysio, PIZZARI, Tania and HONS, Bphysio. Multidirectional instability of the glenohumeral joint : Etiology , classi fi cation , assessment , and management. *Journal of Hand Therapy* [online]. 2017. Vol. 30, no. 2, p. 175–181.

14. YANG, Chen, GOTO, Akira, SAHARA, Wataru, YOSHIKAWA, Hideki and SUGAMOTO, Kazuomi. In vivo three-dimensional evaluation of the functional length of glenohumeral ligaments. *Clinical Biomechanics* [online]. 2010. Vol. 25, no. 2, p. 137–141.

15. HILL, A. M., BULL, A. M.J., RICHARDSON, J., MCGREGOR, A. H., SMITH, C. D., BARRETT, C. J., REILLY, P. and WALLACE, A. L. The clinical assessment and classification of shoulder instability. *Current Orthopaedics*. 2008. Vol. 22, no. 3, p. 208–225.

16. CHARBONNIER, C, CHAGUÉ, S, KOLO, F C, CHOW, J C K and LÄDERMANN, A. A patient-specific measurement technique to model shoulder joint kinematics. *Orthopaedics & Traumatology: Surgery & Research* [online]. 2014. Vol. 100, no. 7, p. 715–719.

17. CALDERONE, Manuela, CEREATTI, Andrea, CONTI, Maurizio and DELLA CROCE, Ugo. Comparative evaluation of scapular and humeral coordinate systems based on biomedical images of the glenohumeral joint. *Journal of Biomechanics*. 2014. Vol. 47, no. 3, p. 736–741.

18. VAN ANDEL, Carolien, VAN HUTTEN, Kim, EVERSDIJK, Marielle, VEEGER, DirkJan and HARLAAR, Jaap. Recording scapular motion using an acromion marker cluster. *Gait and Posture*. 2009. Vol. 29, no. 1, p. 123–128.

19. LABRIOLA, Joanne E., LEE, Thay Q., DEBSKI, Richard E. and MCMAHON, Patrick J. Stability and instability of the glenohumeral joint: The role of shoulder muscles. *Journal of Shoulder and Elbow Surgery*. 2005. Vol. 14, no. 1 SUPPL., p. S32–S38.

20. BROGAN, Kit, BAXTER, Jonathan A. and TENNENT, Duncan. Managing patients with shoulder instability. *Orthopaedics and Trauma* [online]. 2018. Vol. 32, no. 3, p. 153–158.

21. ASKMEN. Flexion and extesnsion for biceps ب. *Anatomical Bicep Training*. 1394.

22. ROBERT-LACHAINE, Xavier, ALLARD, Paul, GODBOUT, Véronique, TÉTREAULT, Patrice and BEGON, Mickael. Scapulohumeral rhythm relative to active range of motion in patients with symptomatic rotator cuff tears. *Journal of Shoulder and Elbow Surgery* [online]. 2016. Vol. 25, no. 10, p. 1616–1622.

23. EBAUGH, D. David, MCCLURE, Philip W. and KARDUNA, Andrew R. Three-dimensional scapulothoracic motion during active and passive arm elevation. *Clinical Biomechanics*. 2005. Vol. 20, no. 7, p. 700–709.

24. SAHARA, Wataru, SUGAMOTO, Kazuomi, MURAI, Masakazu, TANAKA, Hiroyuki and YOSHIKAWA, Hideki. The three-dimensional motions of glenohumeral joint under semi-loaded condition during arm abduction using vertically open MRI. *Clinical Biomechanics*. 2007. Vol. 22, no. 3, p. 304–312.

25. MATSUKI, Keisuke, MATSUKI, Kei O., YAMAGUCHI, Satoshi, OCHIAI, Nobuyasu, SASHO, Takahisa, SUGAYA, Hiroyuki, TOYONE, Tomoaki, WADA, Yuichi, TAKAHASHI, Kazuhisa and BANKS, Scott A. Dynamic in vivo glenohumeral kinematics during scapular plane abduction in healthy shoulders. *Journal of Orthopaedic and Sports Physical Therapy*. 2012. Vol. 42, no. 2, p. 96–104.

26. NISHINAKA, Naoya, TSUTSUI, Hiroaki, MIHARA, Kenichi, SUZUKI, Kazuhide, MAKIUCHI, Daisuke, KON, Yoshiaki, WRIGHT, Thomas W., MOSER, Michael W., GAMADA, Kazuyoshi, SUGIMOTO, Hideharu and BANKS, Scott A. Determination of in vivo glenohumeral translation using fluoroscopy and shape-matching techniques. *Journal of Shoulder and Elbow Surgery*. 2008. Vol. 17, no. 2, p. 319–322.

27. STRUYF, F., NIJS, Jo, BAEYENS, J. P., MOTTRAM, S. and MEEUSEN, R. Scapular positioning and movement in unimpaired shoulders, shoulder impingement syndrome, and glenohumeral instability. *Scandinavian Journal of Medicine and Science in Sports*. 2011. Vol. 21, no. 3, p. 352–358.

28. KOZONO, Naoya, OKADA, Takamitsu, TAKEUCHI, Naohide, HAMAI, Satoshi, HIGAKI, Hidehiko, IKEBE, Satoru, SHIMOTO, Takeshi, MIAKE, Go, NAKANISHI, Yoshitaka and IWAMOTO, Yukihide. In vivo kinematic analysis of the glenohumeral joint during dynamic full axial rotation and scapular plane full abduction in healthy shoulders. *Knee Surgery, Sports Traumatology, Arthroscopy*. 2017. Vol. 25, no. 7, p. 2032–2040.

29. VON EISENHART-ROTHE, Rüdiger, MAYR, Hermann Otto, HINTERWIMMER, Stefan and GRAICHEN, Heiko. Simultaneous 3D assessment of glenohumeral shape, humeral head centering, and scapular positioning in atraumatic shoulder instability: A magnetic resonance-based in vivo analysis. *American Journal of Sports Medicine*. 2010. Vol. 38, no. 2, p. 375–382.

30. MATIAS, Ricardo and PASCOAL, Augusto Gil. The unstable shoulder in arm elevation: A three-dimensional and electromyographic study in subjects with glenohumeral instability. *Clinical Biomechanics*. 2006. Vol. 21, no. SUPPL. 1, p. 52–58.

31. PINKAS, D. and WIATER, J. M. Functional Anatomy of the Shoulder? *Orthopaedic Physical Therapy Secrets: Third Edition*. 2017. P. 318–326.

32. LEVINE, William N and FLATOW, Evan L. The Pathophysiology of Shoulder. *Sports Medicine*. 2000. Vol. 28, no. 6, p. 910–917.

33. LEWIS, Angus, KITAMURA, T. and BAYLEY, J. I.L. (ii) The classification of shoulder

instability: New light through old windows! *Current Orthopaedics*. 2004. Vol. 18, no. 2, p. 97–108.

34. HARRYMAN, Douglas T., SIDLES, John A., HARRIS, Scott L. and MATSEN, Frederick A. Laxity of the normal glenohumeral joint: A quantitative in vivo assessment. *Journal of Shoulder and Elbow Surgery* [online]. 1992. Vol. 1, no. 2, p. 66–76.

35. LEVINE, William N. and FLATOW, Evan L. The pathophysiology of shoulder instability. *American Journal of Sports Medicine*. 2000. Vol. 28, no. 6, p. 910–917.

36. BERGMANN, G., GRAICHEN, F., BENDER, A., ROHLMANN, A., HALDER, A., BEIER, A. and WESTERHOFF, P. In vivo gleno-humeral joint loads during forward flexion and abduction. *Journal of Biomechanics*. 2011. Vol. 44, no. 8, p. 1543–1552.

37. SINS, Lauranne, TÉTREAULT, Patrice, HAGEMEISTER, Nicola and NUÑO, Natalia. Adaptation of the AnyBody™ Musculoskeletal Shoulder Model to the Nonconforming Total Shoulder Arthroplasty Context. *Journal of Biomechanical Engineering* [online]. 2015. Vol. 137, no. 10, p. 101006.

38. EMERY, R. J.H. and MULLAJI, A. B. Glenohumeral joint instability in normal adolescents. Incidence and significance. *Journal of Bone and Joint Surgery - Series B*. 1991. Vol. 73, no. 3, p. 406–408.

39. BIGLIANI LU, KELKAR R, FLATOW EL, POLLOCK RG, Mow VC. Glenohumeral stability. Biomechanical properties of passive and active stabilizers. *Clin Orthop Relat Res*. 1996. Vol. 330, p. 13–30.

40. RATHI, Sangeeta, TAYLOR, Nicholas F., SOO, Brendan and GREEN, Rodney A. Glenohumeral joint translation and muscle activity in patients with symptomatic rotator cuff pathology: An ultrasonographic and electromyographic study with age-matched controls. *Journal of Science and Medicine in Sport* [online]. 2018. Vol. 21, no. 9, p. 885–889.

41. TERRIER, Alexandre, REIST, Adrian, VOGEL, Arne and FARRON, Alain. Effect of supraspinatus deficiency on humerus translation and glenohumeral contact force during abduction. *Clinical Biomechanics*. 2007. Vol. 22, no. 6, p. 645–651.

42. BEAULIEU, C, HODGE, D, THABIT, G, LANG, P, BERGMAN, A and ANONYMOUS. Dynamic imaging of glenohumeral instability with open MRI. *Int. Society for Magnetic Resonance in Medicine*. 1998. Vol. 243, no. 1, p. 1997.

43. BALOGH, Erin P., MILLER, Bryan T. and BALL, John R. *Improving diagnosis in health care*. 2016. ISBN 0309377692.

44. KÖNIG, D P, BERTRAM, C, KAUSCH, T and RÜTT, J. Die klinische Untersuchung der Schulter TT - Clinical Examination of the Shoulder. *Sportverletz Sportschaden*. 1998.

Vol. 12, no. 03, p. 94–101.

45. HETTRICH, Carolyn M., CRONIN, Kevin J., RAYNOR, Martin B., WAGSTROM, Emily, JANI, Sunil S., CAREY, James L., COX, Charles L., WOLF, Brian R. and KUHN, John E. Epidemiology of the Frequency, Etiology, Direction, and Severity (FEDS) system for classifying glenohumeral instability. *Journal of Shoulder and Elbow Surgery* [online]. 2019. Vol. 28, no. 1, p. 95–101.

46. WARBY, Sarah Ann, WATSON, Lyn, FORD, Jon J., HAHNE, Andrew J. and PIZZARI, Tania. *Multidirectional instability of the glenohumeral joint: Etiology, classification, assessment, and management*. 2017. ISBN 0006-0887.

47. MANUSCRIPT, Author. Impingiment.Pdf. . 2012. Vol. 16, no. 1, p. 612–626.

48. BUCHA, Dr. Atul, DASHOTTAR, Dr. Sunita and SHUKLA, Dr. AK. Shoulder MRI in diagnostic evaluation of shoulder joint instability: A comparison with shoulder arthroscopy. *International Journal of Radiology and Diagnostic Imaging*. 2019. Vol. 2, no. 2, p. 23–27.

49. NORDQVIST, Anders and PETERSSON, Claes J. Incidence and causes of shoulder girdle injuries in an urban population. *Journal of Shoulder and Elbow Surgery* [online]. 1 March 1995. Vol. 4, no. 2, p. 107–112. [Accessed 25 April 2020].

50. SHIELDS, David W., JEFFERIES, James G., BROOKSBANK, Andrew J., MILLAR, Neal and JENKINS, Paul J. Epidemiology of glenohumeral dislocation and subsequent instability in an urban population. *Journal of Shoulder and Elbow Surgery*. 1 February 2018. Vol. 27, no. 2, p. 189–195.

51. HINDLE, Paul, DAVIDSON, Eleanor K., BIANT, Leela C. and COURT-BROWN, Charles M. Appendicular joint dislocations. *Injury* [online]. 1 August 2013. Vol. 44, no. 8, p. 1022–1027. [Accessed 25 April 2020].

52. CEREATTI, Andrea, CALDERONE, Manuela, BUCKLAND, Dan M., BUETTNER, Anne, DELLA CROCE, Ugo and ROSSO, Claudio. In vivo glenohumeral translation under anterior loading in an open-MRI set-up. *Journal of Biomechanics* [online]. 2014. Vol. 47, no. 15, p. 3771–3775.

53. YOSHIDA, Masahito, TAKENAGA, Tetsuya, CHAN, Calvin K., MUSAHL, Volker, LIN, Albert and DEBSKI, Richard E. Altered shoulder kinematics using a new model for multiple dislocations-induced Bankart lesions. *Clinical Biomechanics* [online]. 2019. Vol. 70, no. August, p. 131–136.

54. CEREATTI, Andrea, ROSSO, Claudio, NAZARIAN, Ara, DEANGELIS, Joseph P., RAMAPPA, Arun J. and CROCE, Ugo Della. Scapular motion tracking using acromion skin marker cluster: In vitro accuracy assessment. *Journal of Medical and Biological Engineering*. 2015. Vol. 35, no. 1, p. 94–103.

55. CAPPOZZO, a, CATANI, F, DELLA CROCE, U and LEARDINI, a. Position and orietnation in space of bones during movement. *Clin. Biomech.* [online]. 1995. Vol. 10, no. 4, p. 171–178.

56. AMADI, Hippolite O., HANSEN, Ulrich N., WALLACE, Andrew L. and BULL, Anthony M.J. A scapular coordinate frame for clinical and kinematic analyses. *Journal of Biomechanics*. 2008. Vol. 41, no. 10, p. 2144–2149.

57. SAUERS, Eric L., BORSA, Paul A., HERLING, Derald E. and STANLEY, Richard D. Instrumented measurement of glenohumeral joint laxity: Reliability and normative data. *Knee Surgery, Sports Traumatology, Arthroscopy*. 2001. Vol. 9, no. 1, p. 34–41.

58. SAUERS, Eric L., BORSA, Paul A., HERLING, Derald E. and STANLEY, Rick D. Instrumented measurement of glenohumeral joint laxity and its relationship to passive range of motion and generalized joint laxity. *American Journal of Sports Medicine*. 2001. Vol. 29, no. 2, p. 143–150.

59. CRIMMINS, Ian M., MULCAHEY, Mary K. and O'BRIEN, Michael J. Diagnostic Shoulder Arthroscopy: Surgical Technique. *Arthroscopy Techniques* [online]. 2019. Vol. 8, no. 5, p. e443–e449.

60. SHAH, Apurva S., KARADSHEH, Mark S. and SEKIYA, Jon K. Failure of operative treatment for glenohumeral instability: Etiology and management. *Arthroscopy - Journal of Arthroscopic and Related Surgery* [online]. 2011. Vol. 27, no. 5, p. 681–694.

61. HANTES, Michael and RAOULIS, Vasilios. Arthroscopic Findings in Anterior Shoulder Instability. *The Open Orthopaedics Journal*. 2017. Vol. 11, no. 1, p. 119–132.

62. TURRENTINE, Florence E, WANG, Hongkun, SIMPSON, Virginia B and JONES, R Scott. Surgical Risk Factors, Morbidity, and Mortality in Elderly Patients. *Journal of the American College of Surgeons* [online]. 1 December 2006. Vol. 203, no. 6, p. 865–877.

63. WINTHER, Flemming, VIGOUROUX, Corinne, FAYT, André, HORNEMAN, Veli-Matti and ANTTILA, Rauno. ISB recommendations of definitions of joint coordinate systems of various joints for the reporting of human joint motion-part I:anke, hip, and spine. *Journal of Molecular Spectroscopy*. 2002. Vol. 212, no. 2, p. 223–224.

64. MESKERS, C. G.M., VAN DER HELM, F. C.T., ROZENDAAL, L. A. and ROZING, P. M. In vivo estimation of the glenohumeral joint rotation center from scapular bony landmarks by linear regression. *Journal of Biomechanics*. 1997. Vol. 31, no. 1, p. 93–96.

65. STOKDIJK, M., MESKERS, C. G.M., VEEGER, H. E.J., DE BOER, Y. A. and ROZING, P. M. Determination of the optimal elbow axis for evaluation of placement of prostheses. *Clinical Biomechanics*. 1999. Vol. 14, no. 3, p. 177–184.

66. CHARBONNIER, C., CHAGUÉ, S., KOLO, F. C., CHOW, J. C.K. and LÄDERMANN, A. A

patient-specific measurement technique to model shoulder joint kinematics. *Orthopaedics and Traumatology: Surgery and Research* [online]. 2014. Vol. 100, no. 7, p. 715–719.

67. WU, Ge, VAN DER HELM, Frans C.T., VEEGER, H. E.J., MAKHSOUS, Mohsen, VAN ROY, Peter, ANGLIN, Carolyn, NAGELS, Jochem, KARDUNA, Andrew R., MCQUADE, Kevin, WANG, Xuguang, WERNER, Frederick W. and BUCHHOLZ, Bryan. ISB recommendation on definitions of joint coordinate systems of various joints for the reporting of human joint motion - Part II: Shoulder, elbow, wrist and hand. *Journal of Biomechanics*. 2005. Vol. 38, no. 5, p. 981–992.

68. MESKERS, C. G.M., VAN DER HELM, F. C.T., ROZENDAAL, L. A. and ROZING, P. M. In vivo estimation of the glenohumeral joint rotation center from scapular bony landmarks by linear regression. *Journal of Biomechanics*. 1997. Vol. 31, no. 1, p. 93–96.

69. STOKDIJK, M., NAGELS, J. and ROZING, P. M. The glenohumeral joint rotation centre in vivo. *Journal of Biomechanics*. 2000. Vol. 33, no. 12, p. 1629–1636.

70. DE GROOT, J. H. and BRAND, R. A three-dimensional regression model of the shoulder rhythm. *Clinical Biomechanics*. 2001. Vol. 16, no. 9, p. 735–743.

71. HILL, A. M., BULL, A. M.J., DALLALANA, R. J., WALLACE, A. L. and JOHNSON, G. R. Glenohumeral motion: Review of measurement techniques. *Knee Surgery, Sports Traumatology, Arthroscopy*. 2007. Vol. 15, no. 9, p. 1137–1143.

72. PIZZARI, Tania, KOLT, Gregory S. and REMEDIOS, Louisa. Measurement of Anterior-to-Posterior Translation of the Glenohumeral Joint Using the KT-1000. *Journal of Orthopaedic & Sports Physical Therapy*. 2013. Vol. 29, no. 10, p. 602–608.

73. CHARBONNIER, C., CHAGUÉ, S., KOLO, F. C., CHOW, J. C.K. and LÄDERMANN, A. A patient-specific measurement technique to model shoulder joint kinematics. *Orthopaedics and Traumatology: Surgery and Research* [online]. 2014. Vol. 100, no. 7, p. 715–719.

74. KRARUP, Annabel Lee, COURT-PAYEN, Michel, SKJOLDBYE, Bjørn and LAUSTEN, Gunnar S. Ultrasonic measurement of the anterior translation in the shoulder joint. *Journal of Shoulder and Elbow Surgery*. 1999. Vol. 8, no. 2, p. 136–141.

75. SETH, Ajay, MATIAS, Ricardo, VELOSO, António P. and DELP, Scott L. A biomechanical model of the scapulothoracic joint to accurately capture scapular kinematics during shoulder movements. *PLoS ONE*. 2016. Vol. 11, no. 1, p. 1–18.

76. VON EISENHART-ROTHE, Rüdiger, MAYR, Hermann Otto, HINTERWIMMER, Stefan and GRAICHEN, Heiko. Simultaneous 3D assessment of glenohumeral shape, humeral head centering, and scapular positioning in atraumatic shoulder instability: A magnetic resonance-based in vivo analysis. *American Journal of Sports Medicine*. 2010. Vol. 38,

no. 2, p. 375–382.

77. BAHK, Michael, KEYURAPAN, Ekavit, TASAKI, Atsushi, SAUERS, Eric L. and MCFARLAND, Edward G. Laxity testing of the shoulder: A review. *American Journal of Sports Medicine*. 2007. Vol. 35, no. 1, p. 131–144.

78. BOROTIKAR, Bhushan, LEMPEREUR, Mathieu, LELIEVRE, Mathieu, BURDIN, Valérie, BEN SALEM, Douraied and BROCHARD, Sylvain. Dynamic MRI to quantify musculoskeletal motion: A systematic review of concurrent validity and reliability, and perspectives for evaluation of musculoskeletal disorders. *PLoS ONE*. 2017. Vol. 12, no. 12, p. 1–26.

79. SATALOFF, Robert T, JOHNS, Michael M and KOST, Karen M. *Atlas Multiple sclerosis*. 2008. ISBN 978 92 4 156375 8.

80. GEETHANATH, Sairam and VAUGHAN, John Thomas. Accessible magnetic resonance imaging: A review. *Journal of Magnetic Resonance Imaging*. 2019. Vol. 49, no. 7, p. e65–e77.

81. QUENTAL, C., FOLGADO, J., AMBRÓSIO, J. and MONTEIRO, J. A new shoulder model with a biologically inspired glenohumeral joint. *Medical Engineering and Physics*. 1 September 2016. Vol. 38, no. 9, p. 969–977.

82. BERGMANN, G., GRAICHEN, F., BENDER, A., KÄÄB, M., ROHLMANN, A. and WESTERHOFF, P. In vivo glenohumeral contact forces-Measurements in the first patient 7 months postoperatively. *Journal of Biomechanics*. 2007. Vol. 40, no. 10, p. 2139–2149.

83. BUSSE, Harald, THOMAS, Michael, SEIWERTS, Matthias, MOCHE, Michael, BUSSE, Martin W., VON SALIS-SOGLIO, Georg and KAHN, Thomas. In vivo glenohumeral analysis using 3D MRI models and a flexible software tool: Feasibility and precision. *Journal of Magnetic Resonance Imaging*. 2008. Vol. 27, no. 1, p. 162–170.

84. ORTHOPAEDIC, Oxford and CENTRE, Engineering. Bone position estimation from skin marker co-ordinates using global optimisation with joint constraints. *Journal of Biomechanics*. 1999. Vol. 32, p. 129–134.

85. MICHAUD, B., JACKSON, M., ARNDT, A., LUNDBERG, A. and BEGON, M. Determining in vivo sternoclavicular, acromioclavicular and glenohumeral joint centre locations from skin markers, CT-scans and intracortical pins: A comparison study. *Medical Engineering and Physics* [online]. 2016. Vol. 38, no. 3, p. 290–296.

86. HOLZBAUR, Katherine R S, MURRAY, Wendy M. and DELP, Scott L. A model of the upper extremity for simulating musculoskeletal surgery and analyzing neuromuscular control. *Annals of Biomedical Engineering*. 2005. Vol. 33, no. 6, p. 829–840.

87. AMBRÓSIOA, Jorge, QUENTAL, Carlos, PILARCZYK, Bartlomiej, FOLGADO, João and MONTEIRO, Jacinto. Multibody biomechanical models of the upper limb. *Procedia IUTAM* [online]. 2011. Vol. 2, p. 4–17.

88. DICKERSON, Clark R., CHAFFIN, Don B. and HUGHES, Richard E. A mathematical musculoskeletal shoulder model for proactive ergonomic analysis. *Computer Methods in Biomechanics and Biomedical Engineering*. 2007. Vol. 10, no. 6, p. 389–400.

89. SAUL, Katherine R., HU, Xiao, GOEHLER, Craig M., VIDT, Meghan E., DALY, Melissa, VELISAR, Anca and MURRAY, Wendy M. *Benchmarking of dynamic simulation predictions in two software platforms using an upper limb musculoskeletal model* [online]. 2015. Taylor & Francis. ISBN 1476-8259 (Electronic)r1025-5842 (Linking).

90. SAULA, Katherine R., , XIAO HUB, CRAIG M. GOEHLERB, C, , MEGHAN E. VIDTD, E, MELISSA DALYD, E, Anca, VELISARF and , AND WENDY M. MURRAYB, G, H. Benchmarking of dynamic simulation predictions in two software platforms using an upper limb musculoskeletal model. *Comput Methods Biomech Biomed Engin*. 2016. P. 1–26.

91. YAMAGUCHI G.T. *Overview of Dynamic Musculoskeletal Modeling. In: Dynamic Modeling of Musculoskeletal Motion*. Springer. Boston, MA : Springer, 2001. ISBN 978-0-387-28704-1.

92. OPENSIM. Tutorial 3. Scaling, Inverse Kinematics, and Inverse Dynamics. . 2017.

93. PRINOLD, Joe A.I., MASJEDI, Milad, JOHNSON, Garth R. and BULL, Anthony M.J. Musculoskeletal shoulder models: A technical review and proposals for research foci. *Proceedings of the Institution of Mechanical Engineers, Part H: Journal of Engineering in Medicine*. 2013. Vol. 227, no. 10, p. 1041–1057.

94. KUO, A. D. A Least-Squares Estimation Approach to Improving the Precision of Inverse Dynamics Computations. *Journal of Biomechanical Engineering* [online]. 1998. Vol. 120, no. 1, p. 148.

95. SETH, Ajay, SHERMAN, Michael, REINBOLT, Jeffrey A and DELP, Scott L. OpenSim. . 2015. P. 212–232.

96. AURBACH, Maximilian, SPICKA, Jan, SÜSS, Franz and DENDORFER, Sebastian. Evaluation of musculoskeletal modelling parameters of the shoulder complex during humeral abduction above 90°. *Journal of biomechanics* [online]. 2020. Vol. 106, p. 109817.

97. KLEMT, Christian, NOLTE, Daniel, DING, Ziyun, RANE, Lance, QUEST, Rebecca A., FINNEGAN, Mary E., WALKER, Miny, REILLY, Peter and BULL, Anthony M.J. Anthropometric Scaling of Anatomical Datasets for Subject-Specific Musculoskeletal Modelling of the Shoulder. *Annals of Biomedical Engineering*. 2019. Vol. 47, no. 4,

p. 924–936.

98. UNIVERSITY, Stanford. How Inverse dynamics works. [online]. 2018.

99. SEGUIN, A, LEMIEUX, P O, NUNO, N and HAGEMEISTER, N. Simulation of Daily Living Movements With The Anybody Shoulder Model. *10th International Symposium on Computer Methods in Biomechanics and Biomedical Engineering*. 2014. No. April 2012.

100. SINS, Lauranne, TÉTREAULT, Patrice, HAGEMEISTER, Nicola and NUÑO, Natalia. Adaptation of the AnyBody™ Musculoskeletal Shoulder Model to the Nonconforming Total Shoulder Arthroplasty Context. *Journal of Biomechanical Engineering*. 2015. Vol. 137, no. 10, p. 1–7.

101. DAL MASO, Fabien, RAISON, Maxime, LUNDBERG, Arne, ARNDT, Anton and BEGON, Mickaël. Coupling between 3D displacements and rotations at the glenohumeral joint during dynamic tasks in healthy participants. *Clinical Biomechanics* [online]. 2014. Vol. 29, no. 9, p. 1048–1055.

102. HICKS, Jennifer L., UCHIDA, Thomas K., SETH, Ajay, RAJAGOPAL, Apoorva and DELP, Scott L. Is My Model Good Enough? Best Practices for Verification and Validation of Musculoskeletal Models and Simulations of Movement. *Journal of Biomechanical Engineering*. 2015. Vol. 137, no. 2, p. 1–24.

103. ROBERT-LACHAINE, Xavier, MARION, Patrick, GODBOUT, Véronique, BLEAU, Jacinte and BEGON, Mickael. *Elucidating the scapulo-humeral rhythm calculation: 3D joint contribution method* [online]. 2015. Taylor & Francis.

104. XU, Xu, LIN, Jia hua and MCGORRY, Raymond W. A regression-based 3-D shoulder rhythm. *Journal of Biomechanics*. 2014. Vol. 47, no. 5, p. 1206–1210.

105. KARLSSON, D, HÖGFORS, C and PETERSON, B. Biomechanical modeling of the human shoulder. *Journal of Biomechanics* [online]. 1992. Vol. 20, no. 2, p. 157–166.

106. HÖGFORS, Christian, PETERSON, Bo, SIGHOLM, Göran and HERBERTS, Peter. Biomechanical model of the human shoulder joint-II. The shoulder rhythm. *Journal of Biomechanics*. 1991. Vol. 24, no. 8, p. 699–709.

107. BOLSTERLEE, Bart, VEEGER, Dirkjan H.E.J. and CHADWICK, Edward K. *Clinical applications of musculoskeletal modelling for the shoulder and upper limb*. 2013. ISBN 0140-0118.

108. DE GROOT, J. H. and BRAND, R. A three-dimensional regression model of the shoulder rhythm. *Clinical Biomechanics*. 2001. Vol. 16, no. 9, p. 735–743.

109. NIKOOYAN, Ali Asadi, VAN DER HELM, Frans C.T., WESTERHOFF, Peter, GRAICHEN, Friedmar, BERGMANN, Georg and VEEGER, H. E.J. Comparison of two methods for In Vivo estimation of the glenohumeral joint rotation center (GH-JRC) of the patients with

shoulder hemiarthroplasty. *PLoS ONE*. 2011. Vol. 6, no. 3, p. 1–7.

110. BLACHE, Yoann and BEGON, Mickael. Influence of Shoulder Kinematic Estimate on Joint and Muscle Mechanics Predicted by Musculoskeletal Model. *IEEE Transactions on Biomedical Engineering*. 2018. Vol. 65, no. 4, p. 715–722.

111. CARBES, Sylvain. Anybody Shoulder Rhythm. . 2011. No. 26367042, p. 16.

112. SINS, Lauranne, TÉTREAULT, Patrice, HAGEMEISTER, Nicola and NUÑO, Natalia. Adaptation of the AnyBody™ Musculoskeletal Shoulder Model to the Nonconforming Total Shoulder Arthroplasty Context. *Journal of Biomechanical Engineering*. 2015. Vol. 137, no. 10, p. 1–7.

113. WU, Wen, LEE, Peter V.S., BRYANT, Adam L., GALEA, Mary and ACKLAND, David C. Subject-specific musculoskeletal modeling in the evaluation of shoulder muscle and joint function. *Journal of Biomechanics* [online]. 2016. Vol. 49, no. 15, p. 3626–3634.

114. YU, Jay, ACKLAND, David C. and PANDY, Marcus G. Shoulder muscle function depends on elbow joint position: An illustration of dynamic coupling in the upper limb. *Journal of Biomechanics*. 2011. Vol. 44, no. 10, p. 1859–1868.

115. WU, Wen, LEE, Peter V.S., BRYANT, Adam L., GALEA, Mary and ACKLAND, David C. Subject-specific musculoskeletal modeling in the evaluation of shoulder muscle and joint function. *Journal of Biomechanics* [online]. 2016. Vol. 49, no. 15, p. 3626–3634.

116. SAUL, Katherine R. Benchmarking of dynamic simulation predictions in two software platforms using an upper limb musculoskeletal model Katherine. *Comput Methods Biomech Biomed Engin*. 2015. Vol. 18, no. 13, p. 1445–1458.

117. XU, Xu, LIN, Jia Hua and MCGORRY, Raymond W. Coordinate transformation between shoulder kinematic descriptions in the Holzbaur et al. model and ISB sequence. *Journal of Biomechanics*. 2012. Vol. 45, no. 15, p. 2715–2718.

118. XU, Xu, LIN, Jia Hua and MCGORRY, Raymond W. Coordinate transformation between shoulder kinematic descriptions in the Holzbaur et al. model and ISB sequence. *Journal of Biomechanics*. 2012. Vol. 45, no. 15, p. 2715–2718.

119. HOLZBAUR, Katherine R.S., MURRAY, Wendy M. and DELP, Scott L. A model of the upper extremity for simulating musculoskeletal surgery and analyzing neuromuscular control. *Annals of Biomedical Engineering*. 2005. Vol. 33, no. 6, p. 829–840.

120. HÖGFORS, Christian, SIGHOLM, Göran and HERBERTS, Peter. Biomechanical model of the human shoulder-I. Elements. *Journal of Biomechanics*. 1987. Vol. 20, no. 2, p. 157–166.

121. OPENSIM. How inverse kinematic works. [online]. 2018.

122. RANKIN, Jeffery W. Individual Muscle Contributions to Push and Recovery Subtasks during Wheelchair Propulsion. *Journal of Biomechanics*. 2011. Vol. 44, no. 7, p. 1246–1252.

123. OTTEN, E. Inverse and forward dynamics: Models of multi-body systems. *Philosophical Transactions of the Royal Society B: Biological Sciences*. 2003. Vol. 358, no. 1437, p. 1493–1500.

124. SCHAFER, Ronald W. What is a savitzky-golay filter? *IEEE Signal Processing Magazine*. 2011. Vol. 28, no. 4, p. 111–117.

125. STOKDIJK, M., EILERS, P. H.C., NAGELS, J. and ROZING, P. M. External rotation in the glenohumeral joint during elevation of the arm. *Clinical Biomechanics*. 2003. Vol. 18, no. 4, p. 296–302.

126. WESTERHOFF, P., GRAICHEN, F., BENDER, A., ROHLMANN, A. and BERGMANN, G. An instrumented implant for in vivo measurement of contact forces and contact moments in the shoulder joint. *Medical Engineering and Physics*. 2009. Vol. 31, no. 2, p. 207–213.

127. HARI KRISHNAN, R., DEVANANDH, V., BRAHMA, Aditya Kiran and PUGAZHENTHI, S. Estimation of mass moment of inertia of human body, when bending forward, for the design of a self-transfer robotic facility. *Journal of Engineering Science and Technology*. 2016. Vol. 11, no. 2, p. 166–176.

128. SPIEGEL, MURRAY R.; STEPHENS, LARRY J. ESTADÍSTICA/THEORY AND PROBLEMS OF STATISTICS. MCGRAW-HILL, 2009. *Estadística/Theory and problems of statistics* [online]. 2009. ISBN 0071594469.

129. FAVRE, Philippe, SENTELER, Marco, HIPP, Jasmin, SCHERRER, Simon, GERBER, Christian and SNEDEKER, Jess G. An integrated model of active glenohumeral stability. *Journal of Biomechanics* [online]. 2012. Vol. 45, no. 13, p. 2248–2255.

130. CAMPBELL, A. C., LLOYD, D. G., ALDERSON, J. A. and ELLIOTT, B. C. MRI development and validation of two new predictive methods of glenohumeral joint centre location identification and comparison with established techniques. *Journal of Biomechanics*. 2009. Vol. 42, no. 10, p. 1527–1532.

131. SAUL, Kathrine. Benchmarking of dynamic simulation predictions in two software platforms using an upper limb musculoskeletal model Katherine. *Computational Methods Biomechanics Biomedical Engineering* [online]. 2014. Vol. 23, no. 1, p. 1–7.

132. DAL MASO, Fabien, RAISON, Maxime, LUNDBERG, Arne, ARNDT, Anton, ALLARD, Paul and BEGON, Mickaël. Glenohumeral translations during range-of-motion movements, activities of daily living, and sports activities in healthy participants. *Clinical Biomechanics* [online]. 2015. Vol. 30, no. 9, p. 1002–1007.

133. HAJIZADEH, Maryam, MICHAUD, Benjamin and BEGON, Mickael. The effect of intracortical bone pin on shoulder kinematics during dynamic activities. *International Biomechanics* [online]. 2019. Vol. 6, no. 1, p. 47–53.

134. JACKSON, Sherri L. *Research Methods and Statistics A Critical Thinking Approach* [online]. 2009. ISBN 9780495510017.

135. THACKER, Ben H., DOEBLING, Scott W., HEMEZ, Francois M., ANDERSON, Mark C., PEPIN, Jason E. and RODRIGUEZ, Edward a. Concepts of Model Verification and Validation. *Concepts of Model Verification and Validation*. 2004. No. October, p. 41.

9 APPENDIX

9.1 Complementary figures

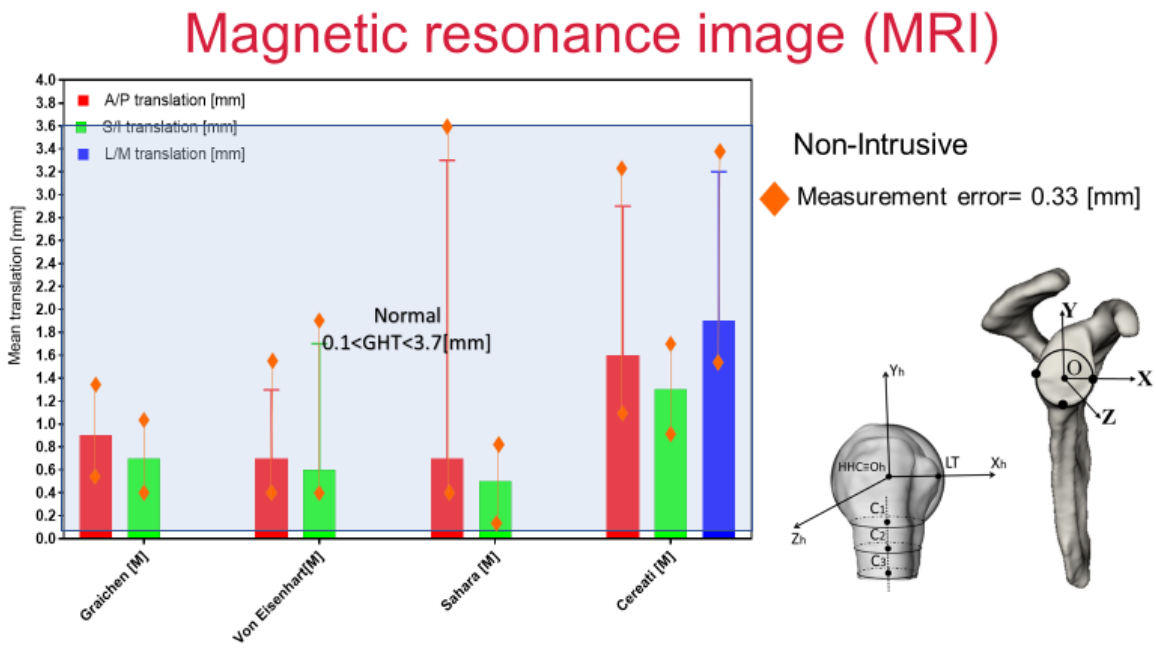

Figure 1. Peak Glenohumeral translations with MRI

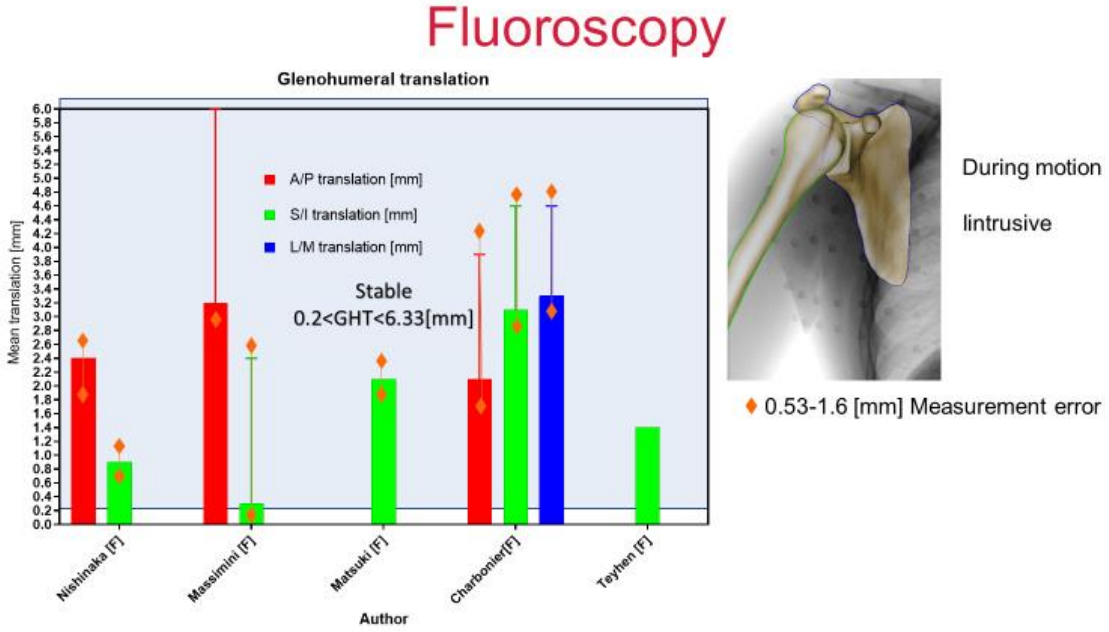

Figure 2.Peak GHJ translations with fluoroscopy

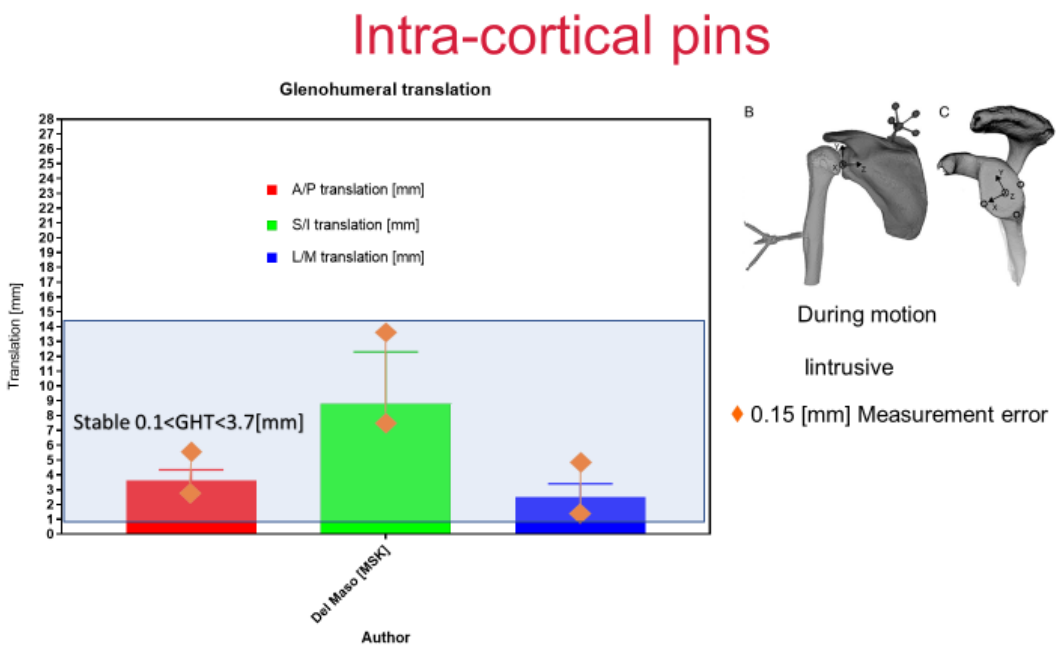

Figure 3. Peak GHJ translations with intra-cortical pins

Coordinate limit force parameters for OpenSim.

Restraint torque CLF						
Coordinate	**upper limit (°)**	**upper stifness (Nm/°)**	**lower _limit (°)**	**lower _stiffness (Nm/°)**	**transition (°)**	**damping (Nm*sec/°)**
shoulder elevation	150	100	30	100	542.8423	0
elevation plane	100	100	−60	100	545.4471	0
shoulder rotation	−10	100	−60	100	485.4660	0
elbow flexion	85	0.3037	14	100	139.5813	0
forearm rotation	60	50	−60	50	430.1186	0
wrist flexion	20	52.5961	−6	487.1760	39.1586	0
wrist deviation	60	200	−60	135.3232	92.9160	0
Damping CLF						
Coordinate ^	upper _limit (°)	upper stifness (Nm/°)	lower _limit (°)	lower _stiffness (Nm/°)	transition (°)	damping (Nm*sec/°)
shoulder elevation	190	0.00000001	190	0.00000001	1	0.001745
elevation plane	190	0.00000001	190	0.00000001	1	0.001745
shoulder rotation	190	0.00000001	190	0.00000001	1	0.001745
elbow flexion	190	0.00000001	190	0.00000001	1	0.001745
forearm rotation	190	0.00000001	190	0.00000001	1	0.001745
wrist flexion	190	0.00000001	190	0.00000001	1	0.001745
wrist deviation	190	0.00000001	190	0.00000001	1	0.0004363

Table 5. Tissue mechanical properties for Holzbaur model [116]

9.2 Glossary

***Verification**: According to the ASME definitions [109]: "*Verification is the process of determining that a model implementation accurately represents the developer's conceptual description of the model and the solution to the model" [135].

Model Validation assessment *:* "Model Validation assessment determines the degree to which a model is an accurate representation of the real world from the perspective of the intended uses of the model" [135].

Root-mean-square deviation (**RMSD**) is used in this thesis as a "measure of the differences between the values that are predicted by a model and the corresponding experimental values", as proposed in [110]